Wet deposition in the remote western and central Mediterranean as a source of trace metals to surface seawater

Karine Desboeufs[1], Franck Fu[1], Matthieu Bressac[2,3], Antonio Tovar-Sánchez[4], Sylvain Triquet[1], Jean-François Doussin[5], Chiara Giorio[6,7], Patrick Chazette[8], Julie Disnaquet [9,10], Anaïs Feron[1], Paola Formenti[1], Franck Maisonneuve[5], Araceli Rodríguez-Romero[4], Pascal Zapf[5], François Dulac[8] and Cécile Guieu[3]

[1] Université de Paris and Univ Paris Est Creteil, CNRS, LISA, UMR 7583, F-75013 Paris, France

[2] Institute for Marine and Antarctic Studies, University of Tasmania, Hobart, Tasmania, Australia.

[3] Laboratoire d'Océanographie de Villefranche (LOV), CNRS-Sorbonne Université, INSU, Villefranche-sur-Mer, 06230, France.

[4] Department of Ecology and Coastal Management, Institute of Marine Sciences of Andalusia (CSIC), 11510 Puerto Real, Cádiz, Spain.

[5] Univ Paris Est Creteil and Université de Paris, CNRS, LISA, UMR 7583, F-94010 Créteil, France

[6] Laboratoire de Chimie de l'Environnement (LCE), UMR 7376 CNRS, Aix-Marseille Université, Marseille, 13331, France.

[7] Yusuf Hamied Department of Chemistry, University of Cambridge, Lensfield Road, CB2 1EW, Cambridge, United Kingdom

[8]Laboratoire des Sciences du Climat et de l'Environnement (LSCE), UMR 8212 CEA-CNRS-UVSQ, Institut Pierre-Simon Laplace, Univ. Paris-Saclay, 91191 Gif-sur-Yvette, France.

[9] Marine Biology Research Division, Scripps Institution of Oceanography, UCSD, USA

[10] Sorbonne Université, CNRS, Laboratoire d'Océanographie Microbienne, LOMIC, France

Correspondence to: Karine Desboeufs (karine.desboeufs@lisa.ipsl.fr)

Abstract. This study reports the only recent characterisation of two contrasted wet deposition events collected during the PEACETIME cruise in the open Mediterranean Sea (Med Sea), and their impact on trace metal (TM) marine stocks. Rain samples were analysed for Al, 12 TMs (Co, Cd, Cr, Cu, Fe, Mn, Mo, Ni, Pb, Ti, V and Zn) and nutrients (N, P, dissolved organic carbon) concentrations. The first rain sample collected in the Ionian Sea (Rain ION) was a typical regional background wet deposition event whereas the second rain sample collected in the Algerian Basin (Rain FAST) was a Saharan dust wet deposition event. Even in remote Med Sea, the background TM inputs presented an anthropogenic signature, except for Fe, Mn and Ti. The concentrations of TMs in the two rain samples were significantly lower compared to concentrations in rains collected at coastal sites reported in the literature, due to the decrease of anthropogenic emissions during the preceding decades. The atmospheric TM inputs were mainly as dissolved forms even in dusty Rain FAST. The TM stocks in the mixed layer (ML, 0-20 m) at the FAST station before and after the event showed that the atmospheric inputs were a significant supply of particulate TMs and of dissolved Fe and Co for surface seawater. Even if the wet deposition delivers TMs mainly as soluble forms, the post-deposition aerosol dissolution could to be a key additional pathway in the supply of dissolved TMs. At the scale of the western and central Mediterranean, the atmospheric inputs were of the same order of magnitude as ML stocks for dissolved Fe, Co and Zn, highlighting the role of the atmosphere in their biogeochemical cycles in the stratified Mediterranean Sea. In case of intense dust-rich wet deposition events, the role of atmospheric inputs as external source was extended to dissolved Co, Fe, Mn, Pb and Zn. Our results suggest that the wet deposition constitutes only a source of some of dissolved TMs for Med surface waters. The contribution of dry deposition on the atmospheric TM inputs need to be investigated.

1. Introduction

Atmospheric deposition of continental aerosol has long been recognized to influence trace element concentrations in remote oceanic surface waters (Buat-Ménard and Chesselet, 1979; Hardy, 1982; Buat-Ménard, 1983). In particular, the Mediterranean Sea (Med Sea) is an oligotrophic environment where marine microbial growth is nutrient-limited during the long Mediterranean summer season, which is characterized by a strong thermal stratification of surface waters (The Mermex Group, 2011). The Mediterranean atmosphere is characterized by the permanent presence of anthropogenic aerosols from industrial and domestic activities around the basin (e.g., Sciare et al., 2003; Kanakidou et al., 2011). In addition to this anthropogenic background, the Mediterranean basin is also subject to seasonal contributions of particles from biomass fires in summer (Guieu et al., 2005) and to intense sporadic Saharan dust inputs (e.g., Loÿe-Pilot and Martin, 1996; Vincent et al., 2016). Several studies have emphasized that the atmospheric deposition of aerosols, notably through wet deposition, plays a significant role in the marine cycles of nutrient, such as nitrogen (N) and phosphorus (P) (e.g. Pulido-Villena et al., 2010; Richon et al., 2018 a and b; Violaki et al., 2018) and micronutrients, such as iron (Fe) (Bonnet and Guieu, 2006). Recently, atmospheric dust inputs were identified to have a fertilizing effect on planktonic stocks and fluxes, even in the presence of relatively high dissolved N, P and Fe concentrations (Ridame et al., 2011; reviewed in Guieu and Ridame, 2021). Mackey et al. (2012) showed that TMs provided by dust deposition could explain this fertilizing effect. Indeed, many TMs, including Mn, Co, Ni (Mackey et al., 2012), Cu (Annett et al., 2008) and Zn (Morel et al., 1991), play physiological roles for phytoplanktonic organisms. These TMs are present in very low concentrations in oligotrophic systems such as the Med Sea, possibly limiting (or co-limiting) phytoplankton growth (Pinedo-Gonzàles et al. 2015) and pointing to the importance of dust deposition as source of TMs for planktonic communities. On the other hand, atmospheric deposition of European aerosols was identified to have a negative effect on chlorophyll concentrations (Gallisai et al. 2014), by providing Cu, at toxic levels (Jordi et al. 2012).

The atmospheric deposition of TMs in the Mediterranean is related to both dust and anthropogenic aerosol deposition (Desboeufs et al., 2018). The role of dust deposition as a source of TMs was observed from the correlation between the atmospheric deposition of mineral dust, and the enrichment of dissolved TMs (Cd, Co, Cu, Fe) in the Med Sea surface microlayer (SML)(Tovar-Sánchez et al., 2014). For the water column, the adding of dissolved Fe and Mn was emphasized in mesocosm experiments after dust addition mimicking intense wet dust deposition (Wuttig et al., 2013). Baconnais et al. (2019) showed that the dissolved Cu isotope signature in surface waters could be related to Saharan dust deposition in the Southern Med Sea. By comparison based on

annual or monthly deposition measurements and marine concentrations, the potential role of atmospheric deposition as source of dissolved Co and Fe for Mediterranean surface waters was also pointed (Bonnet and Guieu, 2006; Dulaquais et al., 2017). Due to Mediterranean sporadic and intense storms, the rain events by scavenging loaded air masses with anthropogenic aerosols or Saharan dust could lead to higher deposition TM fluxes than dry deposition (Desboeufs et al., 2021). Moreover, even if annual wet and dry deposition are equivalent in Mediterranean (Theodosi et al., 2010), wet deposition is known to provide soluble, and potentially bioavailable forms of TMs (Jickells et al., 2016). Yet, to the best of our knowledge, the direct impact of wet deposition on TM concentrations in surface seawater has not been studied in a same location by concurrently collecting both rainwater and seawater samples before this work, whether in the Med Sea or in other oceanic regions.

Two key criteria used to assess the potential impact of TMs and nutrients are their respective concentrations (or fluxes) and fractional solubility (solubility hereafter), i.e., the partitioning between dissolved and total concentrations in rainwaters. Indeed, it is considered that the dissolved fraction of nutrients and TMs is a surrogate for their bioavailability (Jickells et al., 2016). Few studies have reported concentrations of TMs in rainwater samples collected around the Mediterranean basin: Al-Momani et al., (1998), Kanellopoulou, (2001) and Özsoy and Örnektekin, (2009) in the eastern basin, and Losno (1989), Guieu et al. (1997), Frau et al., (1996), Chester et al., (1997) and Guerzoni et al. (1999b) in the western basin. These studies led to highly variable TM concentrations and solubilities, illustrating the large variability of TM inputs during wet deposition events in the Med Sea (reviewed in Desboeufs, 2021). All these studies were performed at coastal sites. Offshore samples of rainwater have rarely been reported in the literature. In the Mediterranean, to our knowledge, trace element concentrations from only three rain samples collected at sea in April 1981 have been reported in a PhD thesis (Dulac, 1986). However, due to the continental and local sources of pollution, the variety of anthropogenic aerosol sources (Amato et al., 2016) and the physico-chemical processes during atmospheric aerosol transport (chemical ageing, dispersion, gravitational settling, in-cloud reactivity..)(Weinzierl et al., 2017), the TM rain composition of the coastal zone may not be representative of atmospheric deposition to the remote Mediterranean.

The PEACETIME cruise (ProcEss studies at the Air-sEa Interface after dust deposition in the MEditerranean Sea) performed in spring 2017 aimed to study the impacts of atmospheric deposition, in particular Saharan dust events, on the physical, chemical and biological processes in this marine oligotrophic environment (Guieu et al., 2020). We investigated the concentration and solubility of TMs and nutrients from two rain events sampled in the central and western Med Sea

during the cruise. We compared our results with the existing literature on TM concentrations in offshore and coastal rain samples dating of 1990's to investigate the time evolution of TM concentrations and the potential differences with the open sea. Additionally, to assess the impact of wet deposition on the surface TM concentrations, surface seawater and rain water were concurrently collected. This is the first time TM data for these atmospheric and marine compartments in Med Sea have all been discussed at the same time and in a same place.

2. Sampling and methods

2.1 Sampling and chemical analysis of rainwater

The PEACETIME oceanographic campaign (https://doi.org/10.17600/17000300) took place in the western and central Med Sea on-board the French R/V *Pourquoi Pas?* between 11 May and 10 June 2017, i.e. at the beginning of the Mediterranean stratification season (Guieu et al., 2020). The rain collector was installed on the upper deck (22 m above sea level) where no on-board activities were taking place to avoid contamination. The rain collector was equipped with an on-line filtration system to separate the dissolved and particulate fractions at the time of collection (details of the filtration system are available in Heimburger et al., 2012) allowing for the calculation of solubility of TMs in the rainwater. The filtration device was equipped with a Nuclepore® polycarbonate membrane filter (porosity: 0.2 μm, diameter: 47 mm). The diameter of the funnel of the collector was 24 cm. The rain collector was installed only when rain was expected and covered by an acid-washed sealed plastic film when not in use. All the sampling materials were thoroughly acid-washed in the laboratory prior to the cruise departure (washing protocol described in Heimburger et al., 2012). No stabilizing device was used to keep the funnel level during the pitch and roll of the ship, preventing a precise assessment of the height of rainfall from the collected water volume. During the rain sampling, the R/V was always facing the wind to avoid contamination by the ship's exhaust, as the chimney was situated on the lower deck and behind the collector.

Immediately after sampling, the collector was disassembled under a laminar flow hood inside an on-board clean-room laboratory. The dissolved fraction was separated into four aliquots dedicated to i) TM determination by inductively coupled plasma coupled methods (ICP), ii) major ion analysis by ion chromatography (IC), iii) dissolved organic carbon (DOC) determination by high-temperature catalytic oxidation (HTCO) on a Shimadzu total organic carbon analyzer (as described in van Wambeke et al., 2021a), and iv) pH measurement. For ICP measurements, the sample was acidified immediately to 1% by volume of ultra-pure nitric acid (67-69%, Ultrapur, Normatom®,

VWR). For IC analysis, the filtrate was immediately frozen. For DOC analysis, the filtrate was collected into pre-combusted glass ampoule and acidified to pH 2 with phosphoric acid. Ampoule was immediately sealed and stored in the dark at room temperature.

The filter (particulate fraction) was dried under the laminar flow hood, and then put in a storage box and packed with a plastic bag to avoid contamination. After returning to the laboratory, filters were acid digested by using the protocol adapted from Heimburger et al. (2012) as follows: filters were placed in tightly capped Savillex™ PFA digestion vessels with 4 mL of a mixture of HNO_3 (67-69%, Ultrapur, Normatom®, VWR), H_2O and HF acids (40%, Ultrapur, Normatom®, VWR) in a proportion of 3: 1: 0.5, then heated in an oven at 130°C for 14 hours. After cooling, the acid solution was completely evaporated on a heater plate (ANALAB, 250, A4) at 140°C for about 2h, then 0.5 mL of H_2O_2 (30-32%, Romil-UpA™) and 1 mL of the acidified water (2% HNO_3) was added to the vessels and heated for 30 min. to dissolve the dry residue in the bottom of the vessels; finally, 12 mL of acidified water (1% HNO_3) was added to obtain 13.5 mL of solution in a tube for ICP analyses.

The dissolved fractions and the solutions issued of digestion of the particulate fractions were analysed by ICP-AES (Inductively Coupled Plasma Atomic Emission Spectrometry, Spectro ARCOS Ametek®, Desboeufs et al., 2014) for major elements (Al, Ca, K, Mg, Na, S) and by HR-ICP-MS (High Resolution Inductively Coupled Plasma Mass Spectrometry, Neptune Plus ™ at Thermo Scientific ™) for P and TMs: Cd, Co, Cr, Cu, Fe, Mn, Mo, Ni, Pb, Ti, V and Zn. The dissolved fraction was analysed by IC (IC 850 Metrohm) for the inorganic and organic anions (NO_2^-, NO_3^-, PO_4^{3-}, SO_4^{2-}, F^-, Cl^-, Br^-, $HCOO^-$, CH_3COO^-, $C_2H_5COO^-$, MSA, $C_2O_4^{2-}$) and for the cation NH_4^+ (Mallet et al., 2017). Only TMs, major nutrients, i.e. N and P species, and Al are discussed in this manuscript. The speciation of dissolved P was estimated by determining dissolved inorganic phosphorus (DIP) from phosphate concentrations expressed as P and the dissolved organic phosphorus (DOP) from the difference between total dissolved phosphorus (TDP), obtained by HR-ICP-MS, and DIP, obtained by IC. The dissolved inorganic nitrogen (DIN) were defined as sum of NO_2^-, NO_3^- and NH_4^+, expressed as N.

In order to estimate the contamination of sampling and analytical protocols, three blanks of rain samples, collected on-board during the cruise, were used and processed. Blank samples were prepared by rinsing the funnel with 150 mL of ultrapure water (18.2 mΩ cm) with the same protocol of rain collection. The procedural limit of detections (LoD) were defined as 3 x standard deviation of blank samples both for dissolved and particulate fractions estimated after acid digestion. All

dissolved and particulate sample concentrations were higher than LoD, except for NO_2^- in the two rain samples. The blank concentrations represented 10.2% on average for TMs and were typically lower than 20% of the sample concentrations, except for Cd (52%) and Mo (43%) in the dissolved fraction. Blank concentrations were subtracted from all sample concentrations.

2.2 Atmospheric ancillary measurements

The PEGASUS (PortablE Gas and Aerosol Sampling UnitS, www.pegasus.cnrs.fr) mobile platform of LISA is a self-contained facility based on two standard 20-feet containers, adapted with air-conditioning, rectified power, air intake and exhausts for sampling and online measurements of atmospheric aerosols and gaseous compounds, and their analysis (Formenti et al., 2019). During the PEACETIME cruise, only the sampling module of the facility was deployed on the starboard side of deck 7 of the R/V. The PEGASUS instrumental payload of relevance to this paper included measurements of the major gases such as NOx, SO_2, O_3 and CO by online analysers (Horiba APNA, APSA, APOA and PICARRO respectively; 2-min resolution, for all gases was detection limit 0.5 ppb and 1 ppb for CO). These gases were used to estimate the origins of sampled air.

From the first of June 2017 (not operational before), additional measurements by an ALS450® Rayleigh-Mie lidar (Leosphere ™; Royer et al., 2011) were used to monitor the vertical distribution of aerosols over time and the associated integrated columns. The vertical lidar profiles were analysed to yield the apparent backscatter coefficient (ABC) corrected from the molecular transmission, as well as the volume depolarisation ratio (VDR). The inversion procedure (Chazette et al., 2016 and 2019) to retrieve the aerosol extinction coefficient (unit km^{-1}) used a vertical-dependent lidar ratio that took into account two aerosol layers. The first layer corresponded to marine aerosols in the marine boundary layer (MBL), the second to a desert aerosol layer that could extend between ~1 and 6 km above mean sea level (amsl). In accordance with Chazette et al. (2016), for the same wavelength and region, the lidar ratios were set to 25 and 55 sr, respectively. The vertical profile of the aerosol extinction coefficient was retrieved from 0.2 km amsl upwards with a vertical resolution of 15 m. Based on these profiles, the integrated column content of dust aerosols was estimated using a specific extinction cross-section of 1.1 m^2 g^{-1} as proposed by Raut and Chazette (2009).

In addition, detailed meteorological data such as air and sea temperature, atmospheric pressure, relative humidity, atmospheric pressure, heat flux and wind speed and direction were provided on a 30 second time step basis by the ship's permanent instrumentation.

2.3 Sampling and analysis of dissolved TMs in seawater

TM samples were also collected in the water column using a titanium trace metals clean (TMC) rosette (mounted with 24 teflon-coated Go-Flo bottles) before and after the rain event (Bressac et al., 2021). Although rosette deployments were performed over the whole water column, we focus here on the 0-20 m marine mixed-layer (ML). Immediately after recovery, the Go-Flo bottles were transferred inside a class-100 clean laboratory container. Seawater samples were directly filtered from the bottles through acid-cleaned 0.2 µm capsule filters (Sartorius Sartobran-P-capsule 0.45/0.2-µm). All samples were acidified on-board to pH<2 with Ultrapure-grade HCl under a class-100 HEPA laminar flow hood. Metals (namely Cd, Co, Cu, Ni, Mo, V, Zn and Pb) were pre-concentrated using an organic extraction method (Bruland et al., 1979) and quantified by ICP-MS (Perkin Elmer ELAN DRC-e) in the home laboratory. The accuracy of the pre-concentration method and analysis for TMs was established using Seawater Reference Material (CASS 6, NRC-CNRC) with recoveries ranging from 89% for Mo to 108% for Pb. Due to the complexity of the analytical method, all the TMC samplings were not analysed for Cd, Co, Cu, Ni, Mo, V, Zn and Pb. Overall, 1 or 2 depths were obtained in the mixed layer (0-20 m). Dissolved Fe and Al concentrations were also measured on-board. Dissolved Fe concentrations were measured using an automated Flow Injection Analysis (FIA) with online preconcentration and chemiluminescence detection (Bonnet and Guieu, 2006), and dissolved Al concentrations using the fluorometric method described by Hydes and Liss (1976). Sampling and analysis for dissolved Fe and Al concentrations are fully described in Bressac et al. (2021), and covered at least four depths in the 0-20 m mixed layer.

2.4 Concurrent sampling strategy

Our sampling strategy of collecting seawater before and after rains were to trace the fate of atmospheric TMs and nutrients in the water column after wet deposition events in an open ocean. The sampling time-resolution was optimized to obtain results before and after rains, however this strategy was very dependent on meteorological conditions. The time chart of the sampling of rain and surface water is presented in Fig. 1.

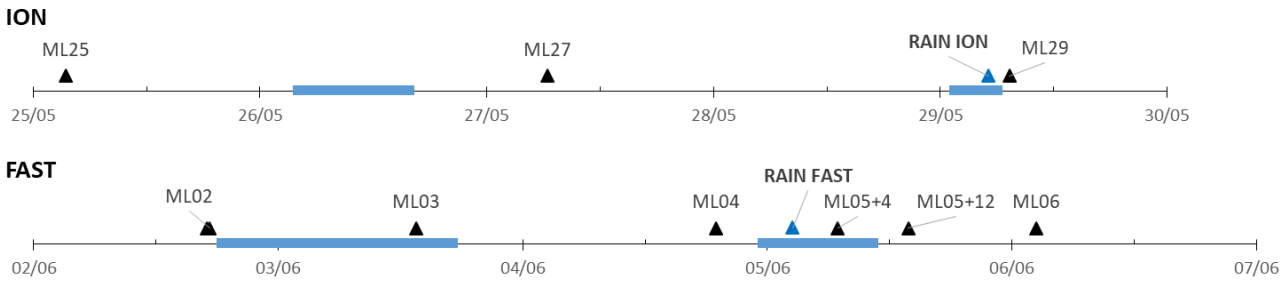

Figure 1: Sampling chronology during the ION and FAST stations for the ML and rains. The blue periods correspond to rainfall in the vicinity of the R/V position (from ERA 5 reanalysis and radar imagery, see section 3.1.), and blue triangles to the rainfall on the R/V position. Samplings were performed 4 days (ML25) and 2 days (ML27) before and 2 h (ML29) after Rain ION, and at a higher frequency at FAST: 57 (ML02), 37 (ML03) and 7.5 (ML04) hours before and 4.5 (ML05+4), 12 (ML05+12), 24 hours (ML06) after Rain FAST.

The potential enrichment of the ML from the Rain FAST was estimated by comparing atmospheric wet deposition fluxes and marine stocks in particulate and dissolved fraction and by calculating the difference (delta) in TM stocks before and after rain. Dust rain deposition over the FAST station area started on 3 June (see section 3.1). Bressac et al. (2021) showed that the dust signature, traced by changes in Al and Fe particulate stocks in the ML, was already visible from the ML03 sampling, but not for dissolved stocks. However, they presumed also that the water mass sampled before deposition (ML02) was different from the one sampled during the rest of the time-series (ML03 to ML06) but was representative of particulate background level. In consequence, we defined the enrichment of seawater layers as the difference between the stocks after rains (ML05+4) and the initial seawater stocks (ML02 for particulate stocks (before dust signature) and ML04 for dissolved stocks (the closest sampling before the rain)).

2.5 Enrichment factor and solubility

In order to better constrain the origin of TMs in the rain samples, their enrichment factors (EF; Rahn 1976) relative to the Earth's crust were calculated based on their total concentrations (dissolved + particulate fractions) as:

$$EF = \frac{([X]/[Al])sample}{([X]/[Al])crust} \quad (1)$$

where $[X]/[Al]$ is the ratio between an element X and Al concentrations in rainwater samples (at the numerator), and in the upper continental crust (denominator) from Rudnick and Gao (2003). Aluminium is currently used as a reference element as it predominantly has a crustal origin. For a

given TM, EF >1 indicates an enrichment with respect to the average composition of the Earth's crust. To account for the soil composition variability of mineral dust sources, TMs with an EF value >10 are considered significantly enriched, which points to a non-crustal source (Rahn, 1976). For most metals, enrichment shows important input from anthropogenic sources, due to their low content in other non-crustal sources such seaspray or biogenic aerosols (Jickells et al., 2016).

The fractional solubility of TMs in the two rainwater events was calculated as:

$$S_X\% = \frac{[X]disssolved}{[X]total} \text{ x } 100 \qquad (2)$$

where $S_X\%$ is the solubility (in %) of an element X in the rainwater, $[X]_{dissolved}$ and $[X]_{total}$ are its soluble and total concentration, respectively.

2.6 Atmospheric wet deposition fluxes

Impacts on biogeochemical cycles and ecosystem functioning following a rain event occur on time scales of a few days (2-3), and space scales of tens of km (about 20-50 km within the radius of the R/V position). In the specific context of oceanographic cruising, the documentation of these impacts is restricted to the vertical dimension at the prescribed temporal scale. In this vertical dimension, the exchange of TMs into the ML was controlled both by atmospheric inputs over the R/V position and by advection from surrounding water masses that may have been impacted by surrounding rainfall. Therefore, we had to consider this process in our estimation of the atmospheric fluxes contributions. For this purpose, the atmospheric fluxes have to be integrated to the extent of the rain area that can impact the marine surface layers. We derived wet deposition fluxes by considering the total precipitation accumulated during the duration of the rain over the area around the R/V position (in a radius of ~25km). Thus, the wet deposition fluxes were calculated by multiplying the TM concentrations (µg L^{-1} or µmol L^{-1}) in our rain samples by the total precipitation (mm) in this area. The total precipitation of the rain events was issued from the hourly total precipitation accumulated during the rain events over the region from ERA5 ECMWF reanalysis (Herbasch et al., 2018) and from the rain rate composite radar products from the European OPERA database (Saltikoff et al., 2019), when it was possible. Although subject to uncertainties (Morin et al., 2003), a surface-based weather radar is probably the best tool to estimate rainfall in the surroundings of the R/V since this method is a direct measurement of precipitation with both a best time and spatial resolution in comparison of model estimations. However, the OPERA database does not include Italian radars, which did not cover the central area of the Ionian Sea during the cruise anyway. ERA5 data were available on regular latitude-longitude grids at 0.25° x 0.25° resolution. The accumulated precipitation was taken from the grid-points spanning the R/V location, ± 0.25° around the central

grid-point for integrating the regional variability. Surface rain rate radar composite images were available every 15 minutes with a spatial resolution of 2 km x 2 km. The accumulated precipitation was the sum of integrated rain rates during the rain duration averaged over the radar pixels spanning the R/V location within a radius of about 25 km around.

2.7 Stocks in the surface seawater

The trace metals stocks within the ML were calculated by trapezoidal integrations of marine concentrations from TMC rosette samplings. The upper water column was stratified along the cruise transect (Taillandier et al., 2020), with a ML depth (MLD) ranging from 7 to 21 m (11 to 21 m at ION and 11 to 19 m at FAST (Van Wambeke et al., 2020). The MLD fluctuations, for example due to wind peaks associated with rain events, could create rapidly changing conditions of vertical advection from deeper waters. However, with no significant increase in TM concentrations being observed below the ML down to about 50 m (not shown), the enrichment observed in the ML after rain could not be attributed to any mixing with deeper water due to high wind. In consequence, stocks in the ML have been integrated over a constant depth range of 0-20 m for comparison, in accordance with Bressac et al. (2021). For Cu, Fe, Ni and Zn, stocks were estimated both for the dissolved and particulate fractions in the ML, for Co, Cd, Mo, Pb and V only for the dissolved fraction (particulate fraction was not analysed) and for Mn and Ti only for the particulate fraction. The particulate and dissolved fractions of TM stock or fluxes will be mentioned as pTM and dTM respectively.

The partitioning coefficient between the particulate and dissolved phases (Kd =[particulate]/[dissolved]) was used to investigate exchange between the dissolved and particulate pools of TMs.

3. Results

3.1 Atmospheric conditions during wet deposition events

The general meteorological conditions during the cruise indicated that the ION and FAST stations were highly affected by cloudy weather conditions. During these periods, two significant rain events occurred over the R/V position and were sampled: The first sample (Rain ION) was collected during the 4-day ION station occupation in the Ionian Sea in the early morning of 29/05/17 at 03:08 UTC. The second rain event (Rain FAST) occurred during the 5-day "Fast action" station occupation,

('FAST') in the Algerian Basin during the night of 05/06/17 at 00:36 UTC (Table 1). The two rain sample collections coincided with peaks in relative humidity and wind speed, and minima in air temperature (not shown).

Table 1: Information regarding the two rains collected during the PEACETIME cruise.

Sample	Sampling time	Station name (dates) and rain location	Estimated total precipitation
Rain ION	29 May 2017, 03:08-04:00 (UTC) 05:08–06:00 (local time)	ION (25–29 May) 35.36°N, 19.92°E	3.5 ±1.2 mm
Rain FAST	05 June 2017, 00:36-01:04 (UTC) 02:36–03:04 (local time)	FAST (2–7 June) 37.94°N, 2.91°E	6.0 ±1.5 mm

3.1.1. Rain ION

The ERA 5 data reanalysis shows two periods of precipitation in the vicinity of the R/V position, i.e. in the morning and evening of 26 June (not shown) and in the night between 28 and 29 June 2017, in agreement with on-board visual observations. The rain event collected at ION was the product of a large cloud system, covering an area of about 90 000 km^2 around the R/V position, spreading over the Ionian and Aegean Seas (Fig. 2). As no radar measurements were available for this area, the accumulated precipitation (3.5 ±1.2 mm) was estimated from ERA 5 data reanalysis on the grid-point corresponding to the ION station (±0.25°) around the R/V position. The wash-out of the atmospheric particles was revealed by the decrease in aerosol number concentrations monitored on-board from about 1900 to 300 $part.cm^{-3}$ (supplementary material Fig. S1). Air mass back-trajectories showed that the scavenged air masses came from Greece both in the marine boundary layer and in the free troposphere (Fig. S1). The satellite observations also showed low aerosol optical thickness during this period (not shown), meaning low amounts of aerosols in the atmospheric column. No significant European pollution influence was monitored by on-board measurements during this event, with major gas mixing ratios and aerosol concentrations close to the average values of the cruise (Fig. S1), i.e. below the limit of detection for NOx, 1.2 ppb for SO_2, 51 ppb for O_3, 80 ppb for CO and 3000 $part.cm^{-3}$. On this basis, this wet event was representative of a Mediterranean background marine rain event.

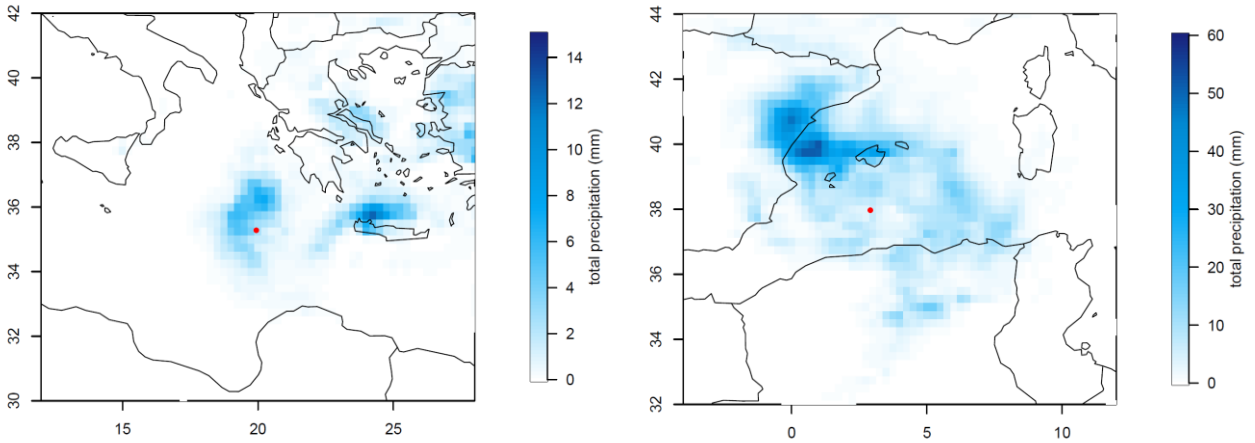

Figure 2: Total precipitation (mm) between 28 May at 20:00 UTC and 29 May 2017 at 10:00 UTC (Rain ION, left figure) and between the 4 June at 20:00 and 5 June 2017 at 09:00 UTC (Rain FAST right figure) from ERA5 ECMWF reanalysis. The red circle indicates the R/V position. Note different scales for total precipitation.

3.1.2. Rain FAST

As detailed in Guieu et al. (2020), the FAST position was decided on the basis of regional model forecast runs and satellite observations, for the purpose of catching a wet dust deposition event. Significant dust emissions were observed from NASCube (http://nascube.univ-lille1.fr/, Gonzales and Briottet, 2017) over North Africa from the night of 30-31 May 2017, then new dust emissions in the night from 3 to 4 June 2017 in Algeria and southern Morocco associated with a northward atmospheric flux. On 30 May, the SEVIRI AOD satellite product (https://www.icare.univ-lille.fr/data-access/browse-images/geostationary-satellites/, Thieuleux et al., 2005) confirmed the presence of atmospheric dust in a cloudy air mass over the western part of the Mediterranean, and from 2 June the export of a dust plume from North Africa south of the Balearic Islands with high AOD (>0.8) on the Alboran Sea was observed (Fig. S2). The dust plume was transported to the NE up to Sardinia on 4 June, with AOD<0.5. Clear sky with low AOD was left west of 4°E on 5 June.

On-board lidar measurements (Fig. 3 a,b,c) showed that the aerosol plume was present over the R/V position from 2 June 2017 at 21:00 UTC until the rain event, and corresponded to a dust aerosol layer highlighted by the high depolarization. The dust plume was concentrated between 3 and 4 km at the beginning of the station occupation, then expanded down to the marine boundary layer (about 500 m amsl) by the end of the day on 3 June 2017. The mass integrated concentrations of dust aerosols derived from the profiles of aerosol extinction ranged from a minimum of 0.18 ±0.005 g

383 m^{-2} just before the rain to a maximum of 0.24 ±0.009 g m^{-2}, where standard deviations indicate the
384 temporal variability (1 sigma).

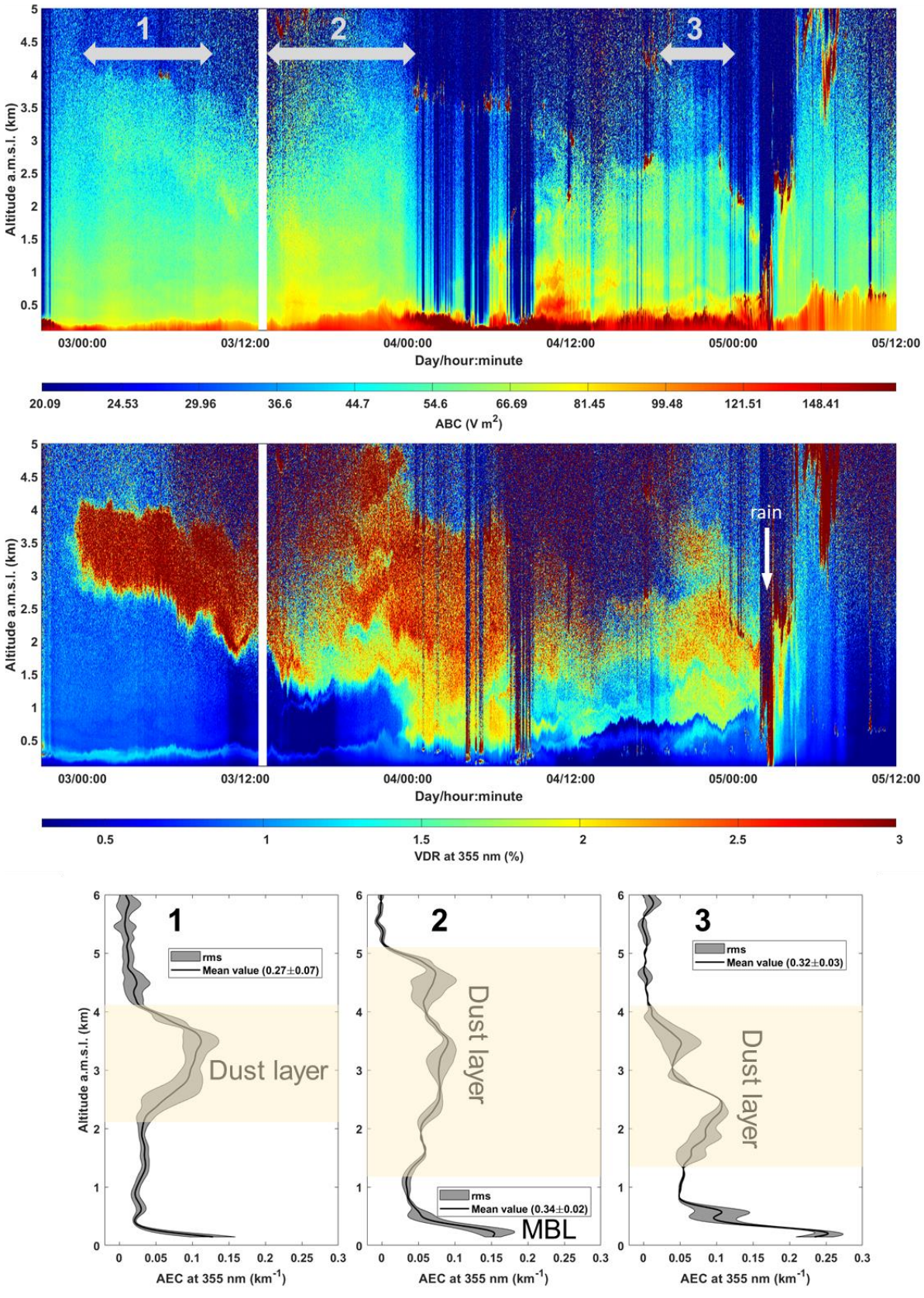

385

Figure 3: On-board lidar-derived: a. apparent backscatter coefficient (ABC) (top panel), b. temporal evolution of the lidar-derived volume depolarization ratio (VDR) (middle panel in local time) where the dust plume is highlighted for values higher than ~1.7 (yellow to red colours) and the rain by values higher than 3 (indicated by the white arrow), and c. vertical profiles of the aerosol extinction coefficient in cloud free condition, integrated over 3 periods, noted 1, 2 and 3 on the top panel, along the dust plume event (bottom panels). The grey shade represents the root mean square (rms) variability along the time of the measurement. The dust layer is highlighted on the profiles. The mean aerosol optical thickness is given in the boxed legend with its temporal variability (1 sigma). The location of the marine boundary layer (MBL) is also pointed.

Rain was observed by weather radar images in the area of the R/V neighbouring from 3 June at 7:00 UTC. The rain recorded around FAST was associated with two periods of rain: from 7:00 to 14:00 UTC on 03/06, and from 16:00 UTC on 04/06 to 06:00 UTC on 05/06. For this latter case, a rain front (100 000 km^2)), moving eastward from Spain and North Africa regions, reached the FAST the night between the 4 and 5 June (Fig. 4). Wet deposition between the 4 and early 5 June in the FAST station area were confirmed by radar imagery, showing several other instances of rain around the R/V position before and after the rain sampling (Fig. 4). Continuous on-board lidar measurements confirmed the below-cloud deposition during the rain event of early 5 June (Fig. 3b). Rain FAST was a wet deposition event occurring at the end of an episode of transport of Saharan dust, whereas precipitation on the 3 June occurred during the maximum of the dust plume (Fig. 3b and S2). The surface concentrations of gas and particles, measured on-board, suggest no clear dust or anthropogenic influence in the atmospheric boundary layer during this period of wet deposition, in agreement with back trajectories of low altitude air masses (Fig S2.), presuming no local mixing between dust and anthropogenic particles into rain samples. The total precipitation estimated from radar rainfall yield an accumulated precipitation of 6.0 ±1.5 mm (±25 km around the R/V position), in agreement with ECMWF reanalysis ERA5 (Fig. 2) for the wet deposition on the night of 4-5 June (5.7 ±1.4 mm in the grid-point spanning the R/V position, i.e. ±0.25°).

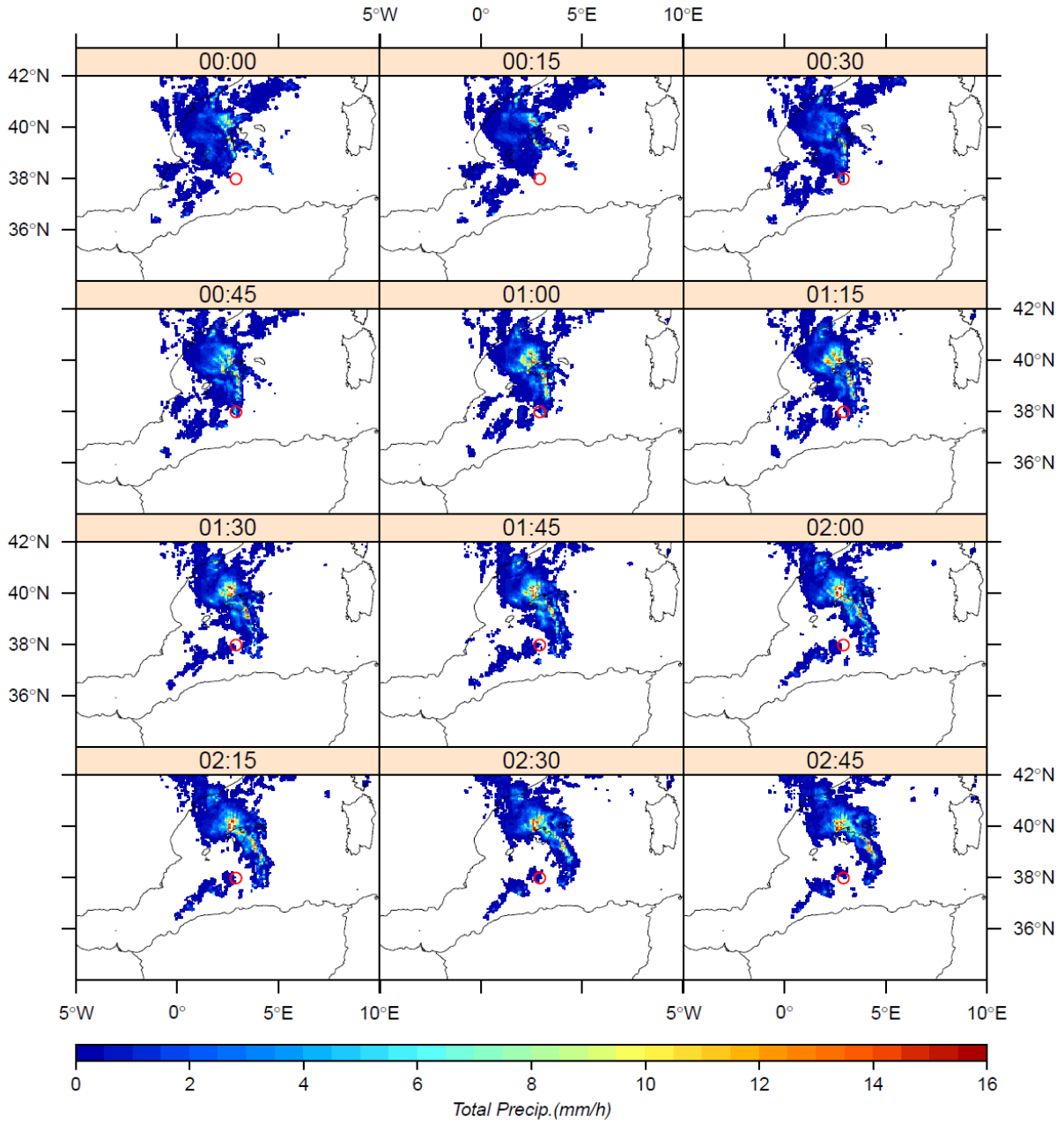

412

413 **Figure 4: Rain rates (mm/h) during the night between the 4 and 5 June, when Rain FAST was collected**
414 **on-board, issued from European rain radar composites (OPERA programme) of 5 June between 00:00**
415 **and 02:45 UTC.**

416 **3.2. Chemical composition of rains**

417 Dissolved and total concentrations of nutrients and TMs in the rain samples are presented in Table
418 2. Among all measured dissolved concentrations, nitrate was the most abundant nutrient, followed
419 by ammonium (Table 2). The nitrite concentration was below the limit of detection for the two rain
420 samples. Regarding TMs in rain, Fe and Zn presented the highest concentrations both in the
421 dissolved fraction and in total deposition with the same order of magnitude (10 to 25 µg L^{-1}). Co,

Cd and Mo had the lowest concentrations (<0.1 μg L^{-1} in both events, associated to the greatest uncertainties due to LoD), whereas the other TM concentrations ranged between 0.1 and 10 μg L^{-1} (Table 2). Concentrations of nutrients and the majority of TMs were higher in the dust-rich rain, except dissolved Pb (similar concentrations in both rain samples) and Cr (3 times higher concentration in Rain ION relative to Rain FAST).

Table 2: Dissolved and total concentrations of nutrients and TMs in the two rain samples collected during the PEACETIME cruise in μg.L^{-1} or ng.L^{-1} and μmol.L^{-1} or nmol.L^{-1} in the parentheses (sd = standard deviation from three replicates).

			Rain ION				Rain FAST			
			Dissolved		Total		Dissolved		Total	
			concentrations	±sd	concentrations	±sd	concentrations	±sd	concentrations	±sd
Nutrients	NO_3^-	μg L^{-1} (μmol L^{-1})	1185 (19.1)	*71 (1.1)*			3694 (59.6	*222 (3.6*		
	NH_4^+	μg L^{-1} (μmol L^{-1})	366 (20.3)	*11 (0.6)*			654 (36.3	*19 (1.1*		
	DIN	μg L^{-1} (μmol L^{-1})	552 (39.4)	*82 (1.7)*			1343 (96)	*241 (17*		
	PO_4^{3-}	μg L^{-1} (nmol L^{-1})	18.1 (189)	*0.5 (6)*			19.0 (200)	*0.6 (6)*		
	DIP	μg L^{-1} (nmol L^{-1})	5.87 (189)	*0.18 (6)*			6.20 (200)	*0.19 (6)*		
	DOP	μg L^{-1} (nmol L^{-1})	8.63 (278)	*1.94 (75)*			4.91 (158)	*1.56 (57)*		
	TP	μg L^{-1} (nmol L^{-1})	14.51 (468)	*2.52 (81)*	16.6 (536)	*1.0 (33)*	11.11 (358)	*1.95 (63)*	58.7 (1894)	*3.5*
	DIN/DIP		(208)				(480)			
	DOC	(μmol L^{-1})	(105.7)	*(2.2)*			(95.5)	*(1.2)*		
Metals	Al	μg L^{-1} (nmol L^{-1})	13.0 (480)	*0.8 (30)*	14.6 (540)	*0.9 (32)*	23.4 (867)	*0.7 (24)*	440 (16308)	*7*
	Cu	μg L^{-1} (nmol L^{-1})	0.71 (11.1)	*0.02 (0.3)*	0.73 (11.5)	*0.02 (0.3)*	1.15 (18.0)	*0.04 (0.6)*	1.63 (25.7)	*0.06*
	Fe	μg L^{-1} (nmol L^{-1})	15.1 (270)	*0.4 (6)*	17.9 (321)	*0.6 (11)*	19.2 (344)	*0.1 (2)*	231 (4140)	*7*
	Mn	μg L^{-1} (nmol L^{-1})	0.55 (10.0)	*0.02 (0.3)*	0.60 (10.9)	*0.02 (0.4)*	3.17 (57.8)	*0.07 (1.2)*	5.26 (95.7)	*0.12*
	Ni	μg L^{-1} (nmol L^{-1})	0.52 (8.8)	*0.02 (0.3)*	0.67 (11.4)	*0.02 (0.4)*	0.59 (10.1)	*0.02 (0.4)*	0.84 (14.3)	*0.03*
	Ti	μg L^{-1} (nmol L^{-1})	0.48 (10.0)	*0.04 (0.8)*	0.65 (13.6)	*0.48 (3.2)*	0.22 (4.7)	*0.01 (0.1)*	33.36 (697)	*0.51*
	V	μg L^{-1} (nmol L^{-1})	0.37 (7.4)	*0.01 (0.2)*	0.38 (7.42)	*0.01 (0.25)*	1.37 (26.9)	*0.03 (0.5)*	2.02 (39.7)	*0.04*
	Zn	μg L^{-1} (nmol L^{-1})	24.8 (379)	*0.8 (12)*	25.3 (387)	*0.8 (12)*	22.7 (347)	*0.6 (8)*	26.3 (402)	*0.7*
	Cd	ng L^{-1} (pmol L^{-1})	12.9 (115)	*6.4 (57)*	13.1 (117)	*6.3 (56)*	20.2 (180)	*10.3 (92)*	23.7 (210)	*6.8*
	Co	ng L^{-1} (pmol L^{-1})	44 (749)	*13 (229)*	47.4 (804)	*14.5 (246)*	82 (1386)	*20 (347)*	157 (2661)	*28*
	Cr	ng L^{-1} (pmol L^{-1})	241 (4636)	*16 (300)*	628 (12079)	*5 (95)*	79 (1522)	*14 (260)*	443 (8514)	*43*
	Mo	ng L^{-1} (pmol L^{-1})	28 (288)	*10 (106)*	4.1 (43)	*1.4 (14)*	82 (855)	*11 (113)*	92.1 (960)	*16.2*
	Pb	ng L^{-1} (pmol L^{-1})	170 (822)	*11 (54)*	175.1 (845)	*1.4 (7)*	166 (801)	*9 (41)*	604 (2917)	*19*

3.3. Marine concentrations

All the TMs had significantly higher concentrations in the ML compared to water below the ML and deeper (e.g. for Fe: Bressac et al., 2021), in agreement with a stratified profile associated with atmospheric inputs. The pTM and dTM concentrations within the ML (0-20 m) are displayed in Fig. 5. Concentrations were of the same order of magnitude at ION and FAST. The TMs were mainly in dissolved forms in the ML (Kd from 0.006 to 0.5), except for Fe (Kd around 2) and one outlier value for Zn (1.3) (Fig. 5).

At both stations, the highest TM concentrations in the surface seawater were found for dMo (~120 nM), these values are the first measurements published in Med Sea and are in agreement with the

high abundance of dMo in open seawater in other oceanic regions (~107 nM, Smedley and Kinniburgh, 2017). Fe is the most abundant in the particulate fraction in the ML (~4 nM). All the pTM and dTM concentrations measured during the cruise were within the range previously published for the Med Sea (Sherrell and Boyle, 1988; Saager et al., 1993; Morley et al., 1997; Yoon et al., 1999; Wuttig et al., 2013; Baconnais et al., 2019; Migon et al., 2020, GEOTRACES-IDP2021). However, dCo concentrations (from 10 to 20 pM) were among the lowest ones measured during stratification period in Western Med Sea (~120 pM, Dulaquais et al., 2017). Zn presented the largest range of concentrations within the ML both in the dissolved and particulate fractions (0.6 to 19 nM and 61 to 3300 pM respectively), due to some high concentrations. However, the concentrations stayed in the typical range of values reported for the Med Sea (Bethoux et al., 1990, Yoon et al., 1999), even if we cannot exclude a possible contamination for these outlier concentrations.

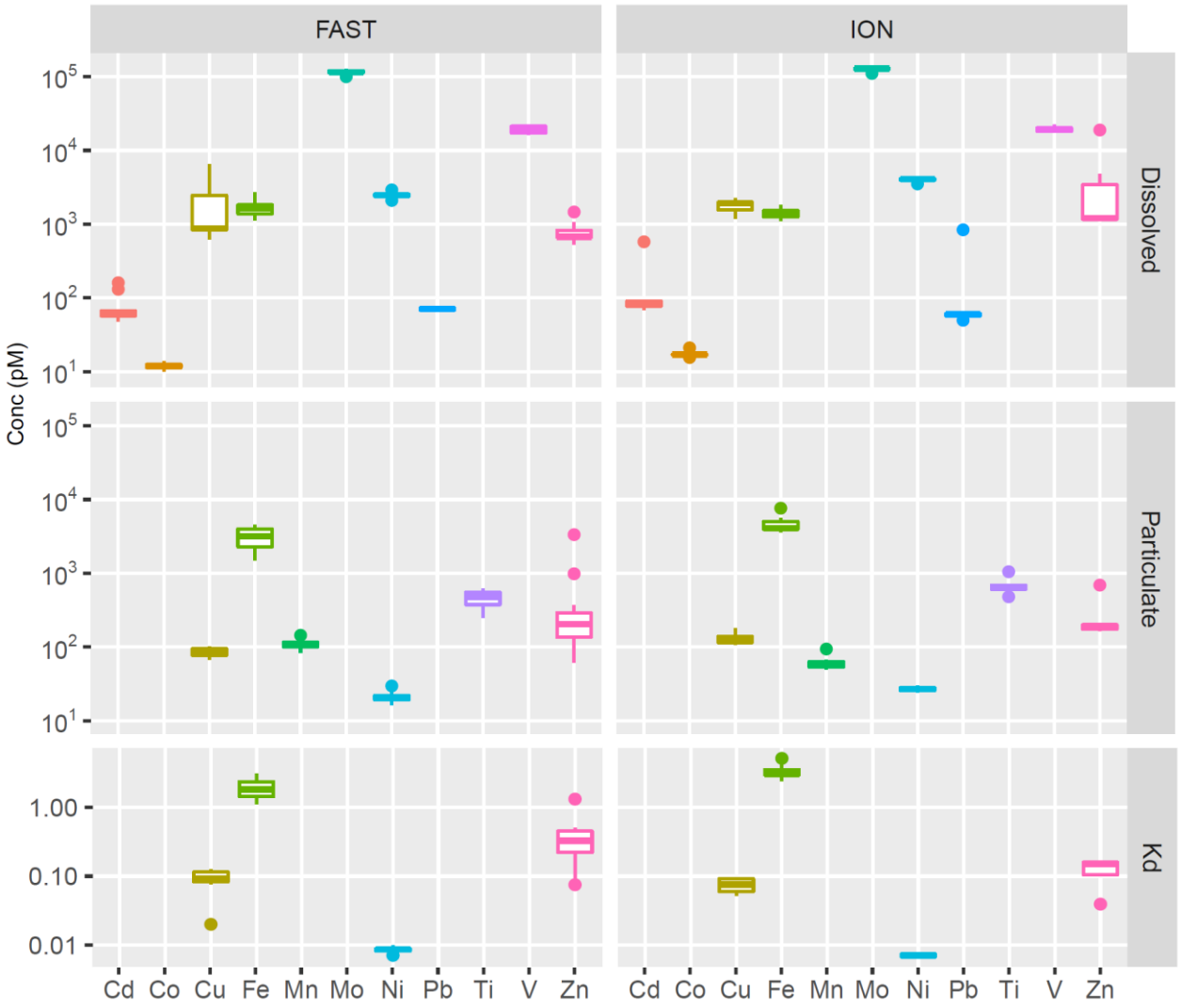

Figure 5: Box plots of dissolved (upper panels) and particulate (middle panels) marine concentrations (pM) and Kd values (lower panels) for the different TMs within the ML at ION (right panels) and FAST (left panels). In the box plots, the box indicates the interquartile range, i.e. the 25th and the 75 th percentile, and the line within the box marks the median. The whiskers indicate the quartiles ±1.5 times the interquartile range. Points above and below the whiskers indicate outliers outside the 10th and 90th percentile.

4. Discussion

4.1. Composition of rain collected over the remote Mediterranean Sea

4.1.1. Concentrations

Regarding nutrients, nitrogen species concentrations in rain samples were in good agreement with those reported in Mediterranean rain samples, ranging from 1130 to 5100 µg L^{-1} for NO_3^- and between 207 and 1200 µg L^{-1} for NH_4^+ (Loye-Pilot et al., 1990; Avila et al., 1997; Al Momani et al., 1998; Herut et al., 1999; Violaki et al., 2010; Izquieta-Rojano et al., 2016; Nehir and Koçak, 2018). The FAST rain concentrations were within the published range, whereas the ION rain was in the low range, confirming a background signature at this station. The rainwater samples presented a large dominance of N in comparison to P, as observed from the N/P ratio derived from DIN/DIP (Table 2) ranging from 208 at ION to 480 at FAST. Previous observations showed a predominance of N relative to P in the atmospheric bulk deposition over the Mediterranean coast, with average ratio about 100, the highest reaching 170 for DIN/DIP and 1200 for DIN/TDP (Markaki et al., 2010, Desboeufs et al., 2018). The highest ratio could be linked to a washout effect of gaseous N species (NOx and NH_3) by rain (Ochoa-Hueso et al., 2011). At the two stations, observed NOx concentrations were below the limit of detection in the boundary layer before wet deposition. The presence of nitrate and ammonium in the background aerosols has been observed during recent campaigns in the remote Mediterranean atmosphere (e.g. Mallet et al., 2019). To our knowledge, no data are available on both P and N concentrations in Mediterranean aerosols. The lowest concentrations of P relative to N in aerosol particles in the Mediterranean were observed during the cruise (DIN/TDP ranged from 13 to 790, Fu et al., in prep.). The TDP concentrations were consistent with the average value of 8.4 µg L^{-1} measured in African dust rain samples collected in Spain over the 1996-2008 period (Izquierdo et al., 2012). Inorganic phosphorus predominated in the dust-rich rain, whereas organic P was dominant in the background rain as the contribution of DOP to the TDP was 60% and 44% in Rain ION and Rain FAST, respectively. The DOP/TDP ratio presents a very large range in Mediterranean rains, spanning from 6% in Spanish dusty rain samples (Izquierdo et

al., 2012) to 75-92% in rains from Crete (Violaki et al., 2018). A reason for this wide range could be that Mediterranean European aerosols, as opposed to Saharan dust particles, are dominated by organic phosphorus compounds associated with bacteria (Longo et al., 2014).

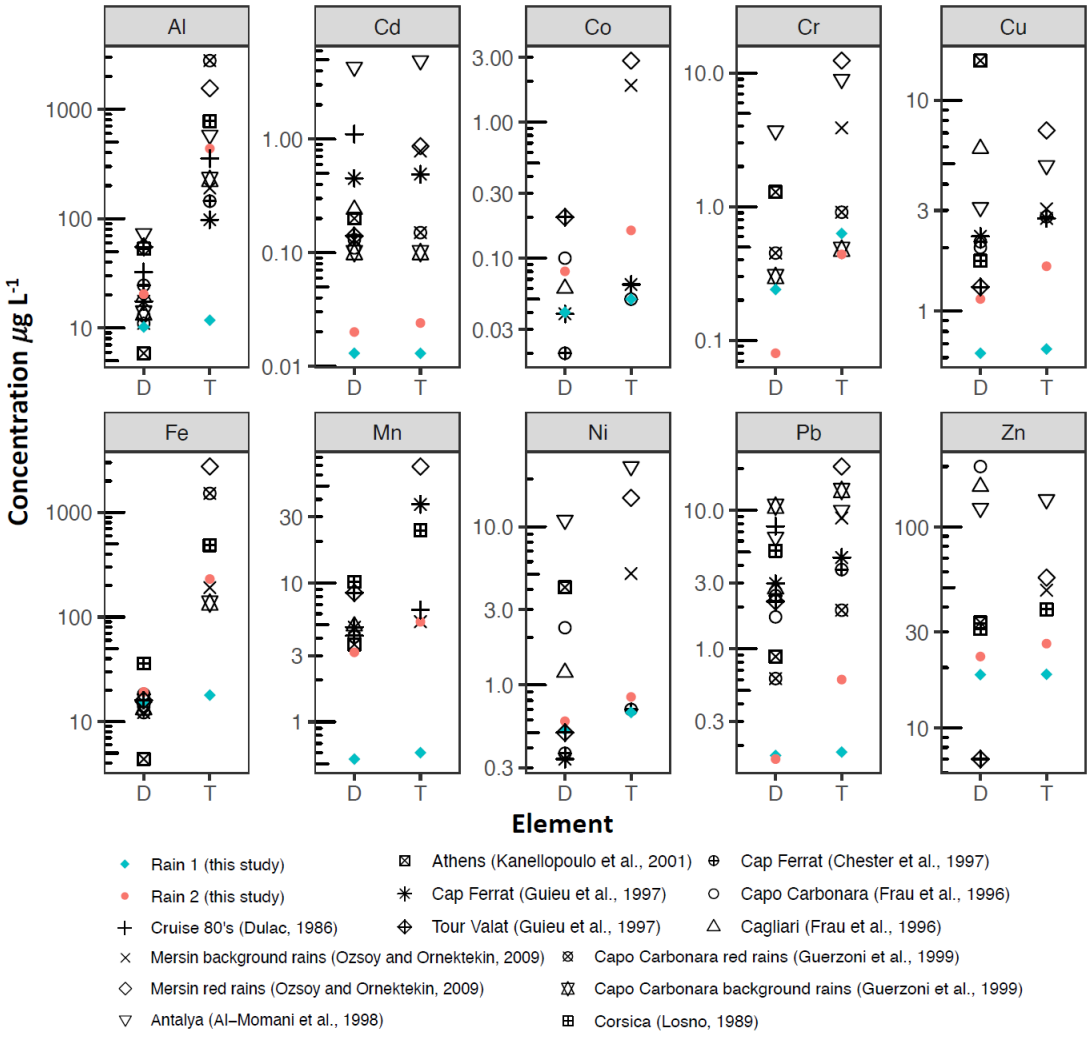

Figure 6: Comparison of dissolved (D) and total (T) TM concentrations to previous studies in the eastern and western Mediterranean Sea.

The dissolved and total TM concentrations in the PEACETIME rains were lower than those reported in coastal areas (eastern Basin: Özsoy and Örnektekin, 2009; Al-Momani et al., 1998; Kanellopoulou et al, 2001 and western Basin: Guieu et al., 1997; Guerzoni et al., 1999b; Chester et al., 1997; Losno, 1989; Frau et al., 1996), especially for the background Rain ION (Fig. 6). Most of the referenced works on coastal rainwaters date from the late 1990s. There is a continuous decline of TM emissions since 90's due to regulatory efforts (Pacyna et al., 2007). The subsequent decrease of the anthropogenic Cd and Pb imprint on atmospheric inputs from European coasts to open sea is well documented (OSPAR, 2008; Travnikov et al., 2012; Geotraces IDP21). Since the phasing-out

of leaded automobile gasoline, the decrease of atmospheric Pb concentrations is also observed in Mediterranean atmosphere (Migon et al., 2008). The low TM concentrations of ION and FAST rain samples, in particular Cd and Pb, suggest a pronounced decrease of TM inputs in open Mediterranean due to environmental mitigation on TM emissions. Moreover, the coastal deposition is generally not representative of open sea inputs, e.g. due to proximity of anthropogenic sources in coastal areas. Thus, the 90's data should not be used as a current reference for open Mediterranean rain composition.

4.1.2. Enrichment factor

EF and solubility values of TMs and P observed during the two rain events were very contrasted (Fig. 7). In Rain ION, almost all elements were significantly enriched relative to the upper continental crust (EF >10, and up to ~10^3 for Cd and Zn), whereas in Rain FAST, only Zn (73), Cd (48) and Mo (15) were enriched. Only Ti, Fe, and Mn did not present a significant enrichment (EF < 10) in Rain ION, in agreement with previous studies in the Mediterranean environment showing that these metals are mainly associated with mineral dust in atmospheric deposition (e.g. Guieu et al., 2010; Desboeufs et al., 2018). Yet, for Fe and Mn, an influence of non-crustal sources in Rain ION could be suspected through a clear increase in the EF values compared to FAST. Mo is the most abundant TM in seawater (Smedley and Kinniburgh, 2017) and in particular in Med Sea (see section 3.3). Thus, at the difference of other TMs, the non-crustal part of Mo could be associated to seasalt aerosols rather than anthropogenic signal. The EF ratio relative to seawater ($(Mo/Na)_{seawater}$ = 8.9 10^{-7} in mass ratio, Millero, 2013) were 7.4 for Rain ION and 4.6 for Rain FAST confirming the marine origin of this element in both rain samples. The anthropogenic origin of TMs and P have been reported by several studies on atmospheric deposition monitoring in the western Mediterranean (e.g., Guieu et al., 2010; Sandroni and Migon, 2002; Desboeufs et al., 2018). For example, Desboeufs et al. (2018) showed that there is a large contribution of anthropogenic combustion sources to the P, Cr, V and Zn background deposition fluxes. Aerosol composition monitoring over the Mediterranean coastal area showed the role of land-based sources and ship traffic sources on TM contents (Bove et al., 2016; Becagli et al., 2017). As all the deposition measurements sites were located in coastal areas, it was difficult to exclude the influence of these local sources for explaining the observed anthropogenic contribution. Here, EF values showed a clear anthropogenic signature for P and all TMs except Ti, Fe, Mn and Mo in the offshore Rain ION sample. In particular, the EF of Zn in Rain ION was on average five times higher than the EF found in the rain samples previously studied from coastal sites in the Mediterranean region (Özsoy and Örnektekin, 2009; Al-Momani et al., 1998; Losno, 1989). Nevertheless, extremely high enrichments

of Zn in rainwater have been reported from island sites in the Med Sea, for example Frau et al. (1996) reported geometric mean EF of ~6500 in both dust-rich and dust-poor rains from two sites in southern Sardinia, and Fu et al. (2017) reported EF >1000 for Zn in atmospheric insoluble bulk (wet+dry) deposition on Lampedusa Island. As previously discussed (section 3.1.1.), Rain ION was representative of a Mediterranean background marine rain event. The Zn EF at ION was the same order of magnitude as at these island sites which suggests a high anthropogenic background signal of Zn even in open Med. More generally, the high EFs in Rain ION mean that even over the remote Med Sea, the chemical composition of background aerosol particles is likely continuously impacted by anthropogenic sources.

The EF values of TMs for Rain FAST were significantly lower than for Rain ION (Fig. 7) but similar to Saharan rains (Guerzoni et al., 1999b; Özsoy and Örnektekin, 2009), confirming the dust signature for this rain. The comparison between dust-rich and background rains generally reveals a net difference of concentrations (at least higher by a factor 3 in dust-rich), notably for Al, Fe, Mn and Cr (Guerzoni et al., 1999b; Özsoy and Örnektekin, 2009). Here, an increase in concentrations between rains ION and FAST was observed for the majority of TMs: Al (x28), Ti (x50), Mo (x23), Fe (x13), Mn (x9), V (x5), Pb (x3.5), Co(x3) and Cu (x2) but also for P(x4) (Table 2). The combination of higher concentrations and EF values <10 found in Rain FAST show that the dust contribution was important on deposition fluxes of many TMs and P during this event. However, the high Al concentrations in rain FAST drives mathematically down EF values, masking potentially other source signature.

4.1.3. Solubility

The solubility values were also higher in Rain ION than in the dusty Rain FAST, except for Mo for which the difference between both rain samples was not significant (Fig. 7). For Rain ION, TMs and P presented solubility higher than 78%, except for Cr (38%). In Rain FAST, solubility values <10% were observed for Al and Fe, more than 10 times lower than in Rain ION. For the other TMs, the highest difference in solubility was observed for Pb whose solubility decreased from 97% in Rain ION to 27% in Rain FAST. In a review on TM solubility in Mediterranean rainwaters collected in coastal areas, Desboeufs (2021) emphasize the large range of solubility for all the TMs: Fe (0.8-41%), Cr (6-80%), Pb (5-90%), Ni (22-93%), Mn (16-95%), Cu (22-96%), Zn (14-99%), V (35-99%) and Cd (72-99%). The solubility ranges found in this study were generally consistent with those reviewed by Desboeufs (2021). Moreover, the Mn solubility values in FAST (60%) and ION (92%) rains are close to those reported by Dulac (1986) from a dust-rich (57%) and an

anthropogenic (83%) rain collected at sea in the Ligurian Sea and west of Sardinia in April 1981. Only Fe solubility (84%) found in Rain ION was higher than the average values previously reported. In the Rain FAST, Fe solubility was 8%, this is 10 times lower than the average Fe solubility in 10 dust-rich rains collected on the southeastern coast of Sardinia by Guerzoni et al. (1999b), but consistent with Saharan dust deposition collected in the Atlantic Ocean (Sedwick et al., 2007; Baker et al., 2013). It is known that anthropogenic Fe is more soluble than Fe-bearing dust (Desboeufs et al., 2005, Jickells et al., 2016). Regarding the evolution of TM emissions (see section 4.1.1), we suspect that this difference could be due to a higher contribution of anthropogenic signal for Fe in dust-rich rains in 90's in Sardinia that in the recent rain samples.

Figure 7: Enrichment Factors (EF, upper panel) and solubility (%, bottom panel) of phosphorus (P) and TMs ordered by increasing EF in the two rainwater samples.

Few studies have compared TM solubility between dust-rich and anthropogenic rains in Mediterranean. An increase in solubility values from dust-rich to background rains was observed for Mn in offshore rains as mentioned above (Dulac, 1986) and for Al, Cr, Fe and Pb (but only a slight increase for Cd) in Sardinia (Guerzoni et al., 1999b). The decrease in solubility from background to dust-rich rains was observed for P in Spain by Izquierdo et al. (2012), with values of

581 solubility decreasing from 25% to 7%. Here, our results on the two rain samples confirm the lowest
582 solubility of TMs in dust-rich rains (except for Mo). Aerosol leaching experiments showed that
583 metal dissolution from aerosol particles can be also influenced by a number of parameters, such as
584 pH, presence of dissolved organic complexing ligands, in-cloud processing, particle origin and load
585 (Desboeufs et al., 1999; Bonnet and Guieu, 2004; Desboeufs et al., 2005; Paris and Desboeufs,
586 2013; Heimburger et al., 2013, Jickells et al., 2016). However, it is known that metals that are
587 mainly associated with crustal aluminosilicate mineral lattices such as Fe and Ti have very low
588 solubility values, due to the difficulties to breaking bonds in the lattices (Jickell et al., 2016).
589 Regarding metal partitioning in rainwater, the role of pH and of the particulate mineral dust loading,
590 reflecting the dust versus anthropogenic signature, were identified as the main controls of TM
591 solubility in the Mediterranean rainwater (Özsoy and Örnektekin, 2009; Theodosi et al., 2010).
592 From our two rain samples, it is difficult to propose a control explaining the difference in solubility
593 values. However, the pH values were very close in the two samples (Table 2), excluding a pH effect
594 on solubility values. A much lower solubility of TMs in Rain FAST is consistent with the EFs
595 indicating a crustal origin of TMs in Rain FAST (Fig. 7). As discussed before, background
596 atmosphere in Med Sea seems to be continuously influenced by anthropogenic particles. Even in
597 dusty-rain FAST, it is highly probable that a part of metals presented an anthropogenic imprint, not
598 visible on EF values but with solubility similar than in Rain ION. Thus, the decrease of solubility
599 between the two rain samples could be either due to the lowest solubility of TMs in mineral dust
600 (as suggested by aerosol leaching experiments), either results from the presence of mineral dust
601 which by increasing the TM total concentrations overwhelms the anthropogenic background signal,
602 or both. The case of Mo is unique, since its solubility was comparable in Rains ION and FAST. As
603 discussed from EF values Mo was associated to seasalt aerosols in both rain samples, explaining
604 the similarity of solubility.

605 **4.2. Atmospheric wet deposition as a source of TMs to the surface seawater**

606 *4.2.1. Atmospheric fluxes*

607 As mentioned before, the two collected rains were part of large rain systems, associated with patchy
608 rainfalls that lasted several hours or days (see section 3.1). This spatio-temporal variability led to
609 heterogeneity in both rainwater concentrations and accumulated precipitation across the studied
610 region. Such spatial variability has been observed by Chance et al. (2015) in the Atlantic Ocean.
611 Moreover, even weak lateral advection can transfer surface water impacted by intense precipitation
612 in the vicinity of the vessel. On this basis, the spatial extrapolation of wet deposition fluxes seems

subject to large uncertainties (almost 100% RSD) when the rain samples are not collected across the rain area (Chance et al., 2015). To best counteract this effect, spatial variability was taken into account to quantify the total precipitation i.e. 3.5 ±1.2 mm for rain ION and 6.0 ±1.5 mm for rain FAST (see section 3.1) in order to quantify the wet deposition fluxes (here ~25% RSD for total precipitation and 1 to 74% RSD for concentrations).

From the total (dissolved + particulate) Al concentration measured in the Rain FAST sample, we estimated the wet mineral dust deposition flux at 65 ±18 mg m^{-2}, assuming 7.1% Al in dust (Guieu et al., 2002). The vertical distribution of dust particles (Fig. 3b) and the absence of high Al concentrations close to the sea surface (Fu personal comm.) indicate that dust dry deposition can be neglected. Based on the increase in total Al in the upper 20 m of the column water following the deposition events and using 7.1% for Al in dust, Bressac et al. (2021) derived an average dust deposition flux of ~55 mg m^{-2} at FAST, which is comparable to our estimate. Although low compared to deposition fluxes reported in the western Mediterranean (Bergametti et al., 1989; Loÿe-Pilot and Martin, 1996; Ternon et al., 2010), our flux estimates are in the same order of magnitude of the most intense weekly dust deposition fluxes calculated more recently in Corsica between 2011 and 2013 (14% of fluxes >50 mg m^{-2}) and is comparable to the mean weekly flux (93 mg m^{-2}) reported for Majorca during the same period (Vincent et al., 2016). The columnar aerosol concentration during the dust event at FAST being estimated to be between 0.18 and 0.24 g m^{-2} (see section 3.1.), the expected maximum values of atmospheric dust flux could be in this range. The comparison with the estimated flux indicates that the atmospheric column was probably not totally washed-out by the short rain event. Indeed, Fig. 3b shows that a significant depolarization was observed immediately after the rain ended on the R/V, before atmospheric advection could have brought dusty air possibly not affected by rain. Satellite products (Fig. S2) confirm that on 5 June, the dusty air mass was transported farther to the north-east from the station where it was replaced by clear air.

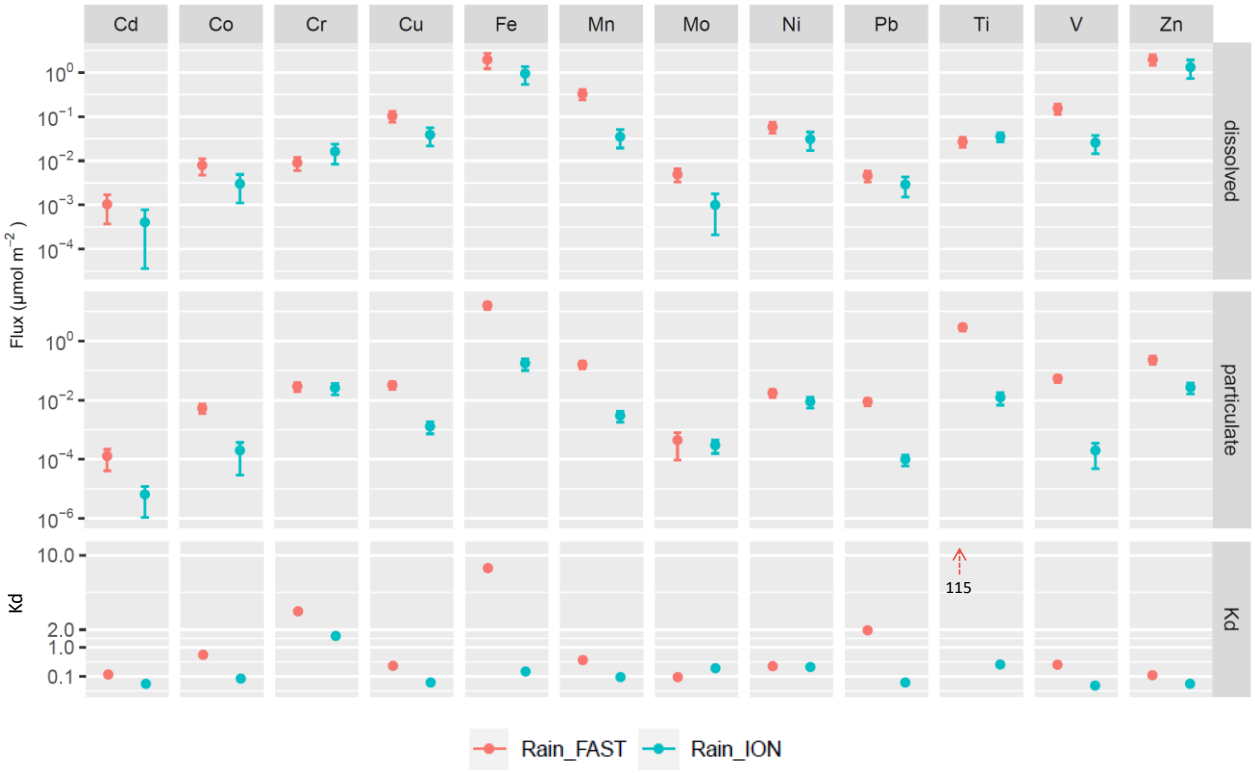

Figure 8: Dissolved (upper panels) and particulate (middle panels) wet deposition fluxes (µmol m^{-2}), and Kd (lower panels) for the different TMs estimated from the two rains sampled on-board, considering the standard deviation on the TM concentrations and the spatial variability of total precipitation over the area of sampling (Rain ION in blue and Rain FAST in red). Note different scales on the y axes and that Kd value for Ti (115) in Rain FAST is out of scale.

The atmospheric dissolved and particulate wet deposition fluxes of TMs, derived from the chemical composition and total precipitation of rain samples, are presented in Fig. 8. Co, Mo and Cd presented the lowest fluxes in the two rainfalls. Zn and Fe fluxes were on the same order of magnitude and were the highest dissolved fluxes compared to the other TMs in the two rains. The Kd values (0.1< Kd <1), in consistence with solubility values higher than 50% (Fig. 7), show that whatever the rain sample, the atmospheric TM inputs were, mainly dissolved, except Fe, Pb and Ti in Rain FAST and Cr in the two rains (Fig. 8). The comparison shows that almost all the dTM fluxes were higher in the dusty rain, except Cr and Ti due to their low solubility in Rain FAST. Our results suggest that dust deposition resulted in higher atmospheric inputs of TMs than from low perturbed-anthropogenic background rain, even here in the case of the moderate deposition input flux reported. With more than an order of magnitude difference in deposition fluxes in the two rain events, this most notably be the case for particulate Fe, Mn, Pb and Ti, typically poorly soluble from desert dust source. Dissolved Cd, Co, Cu, Mn and V fluxes present the highest increases between background

Rain ION and dusty Rain FAST. Yet, these former elements (except Mn) are usually considered issued from anthropogenic sources. The orders of magnitude found in this study could be used as a benchmark to estimate atmospheric inputs of TMs from wet deposition to the western Med Sea. However, we must keep in mind that annual and long-term deposition fluxes of desert dust-related elements, as Fe, Mn and Ti (e.g. Ternon et al., 2010), but also nitrogen species (e.g., Richon et al., 2018b), are dominated by a few atypical intense deposition events in the Med Sea, as is the case in many other oceanic regions (Duce et al., 1991).

4.2.2. Comparison between TM wet deposition inputs and marine stocks at FAST

As previously discussed, the atmospheric concentrations measured in this study were the most recent measurements in remote Med Sea, and were inferior to 90's measurements in coastal zone. As described in Guieu et al. (2020), marine dynamic conditions at FAST were favourable to observe any change in the water masses strictly attributed to external inputs coming from the atmosphere on a short time scale. The impact of the dust wet depositions on nutrients stocks in the Mediterranean surface waters is discussed in details in van Wanbeke et al. (2020) and Pulido-Villena et al. (2021). To briefly summarise, both nitrate and DIP increased in the ML following the rain. Although the closure of the N and P budgets had to necessarily take into account post-deposition processes such as new nutrient transfer through the microbial food web (uptake, remineralisation, and adsorption/desorption processes on sinking particles), it was shown that wet deposition was a significant source of nutrients for the ML during the cruise. For example, atmospheric supply of phosphate could contribute to 90% of new production at FAST (Pulido-Villena et al., 2021). Bressac et al. (2021) studied the response to Al and Fe cycles to dust deposition during the cruise. They showed that total Fe and Al stocks were increased by dust wet deposition, and that the dissolved Fe atmospheric inputs were transient in the ML and were accumulated in the subsurface waters (100-1000m). The low depth-resolution of marine TM concentration samplings prevent the possibility to make TM inventories on the water column. We focus here on the role of dust wet deposition events as a source of TMs to the surface mixed-layer, except Mo due its marine origin in the rain samples. The deltas of TM stocks before and after Rain FAST compared to the atmospheric fluxes are presented in Fig. 9.

After Rain FAST, ML stocks increased for pFe (+61%), pMn (+15%), pTi (+23%) and pZn (+9%) and for dCo (+6%) and dFe (+46%) (Fig. 9). The behaviour of pFe, pMn, pTi and pZn is consistent with observations on pAl stock which increased by 78% after rain (Bressac et al., 2021). The atmospheric particulate inputs were higher to the marine particulate deltas for all the TMs (Fig. 9),

supporting that the marine stock increases resulted from atmospheric inputs. The pTM inputs by rain was also observed from Kd increase in the ML for Fe (1.7 to 1.9) and for Zn (0.33 to 0.57), in agreement with the highest Kd values in rain fluxes (Fig. 7) relative to marine ratio (Fig. 4). The increase Kd was even observed for Cu (0.044 to 0.091) and Ni (0.0081 to 0.0086) for which no change in stock could be evidenced. It is probable that the rain inputs for these TMs be masked in the uncertainties of stock estimations. As dissolved concentrations of Mn and Ti were not measured in the ML, it is not possible to estimate the Kd values. However, the particulate Mn/Al ratio fell from 0.27 before the rain to 0.008 after rain, in accordance with the rain ratio (0.002), confirming the impact of rain inputs on marine particulate stocks of Mn and Al. For Ti, the particulate Ti/Al ratios were very close in the ML (0.048) and in the rain (0.045), making it impossible to observe a rain effect. Here, the observed deltas were inferior to the rain inputs. However, the marine sampling were 4h after rain. Bressac et al. (2021) showed a decrease of 40% of pAl signal in 24h which could be explained either by a rapid settling of dust in the ML, or by lateral advection. The dynamic of pFe, pMn and pTi stocks, with a decrease with time after rain (not shown), is consistent with dust removal in the ML. The pCu and pNi inputs represented 4% and 10% of particulate marine stocks. The dust removal could overwhelm the signal of enrichment of these metals. However, we cannot exclude that the pCu and pNi inputs were masked by the uncertainties of stock calculations.

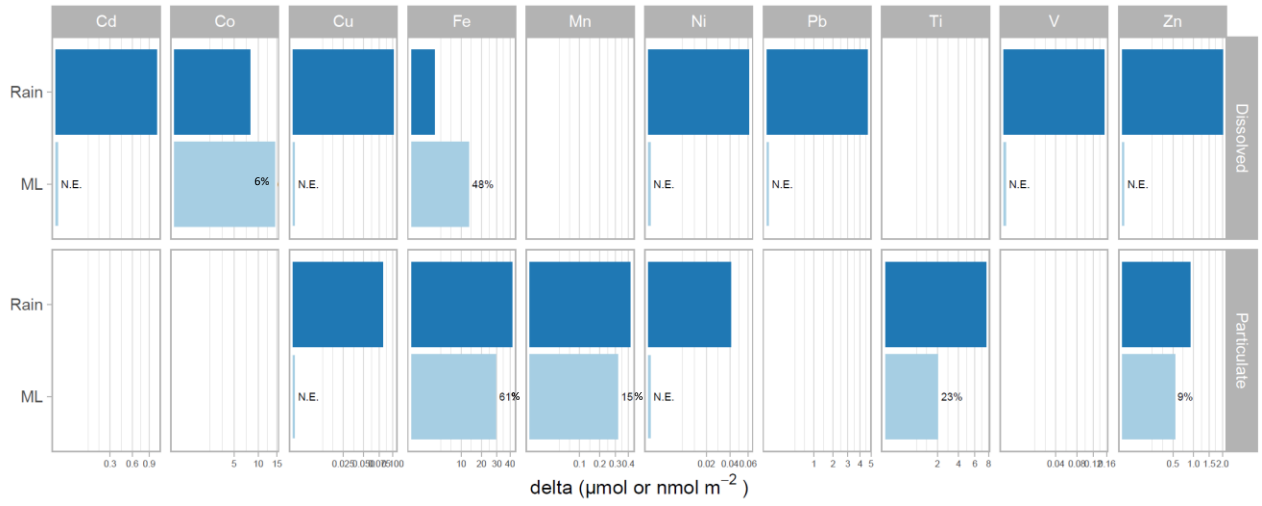

Figure 9: Comparison between TM wet deposition fluxes (dark blue) and TM marine stock deltas (before and after the rain) in the ML (light blue) at FAST. Dissolved = upper panels and particulate = lower panels. Marine stocks increase are expressed in absolute values (Cd, Co and Pb stocks and fluxes in nmol m^{-2}, and the other TMs in µmol m^{-2}) and in relative values (%). N.E.: not enhanced (increase <5%).

For dissolved stocks, no enrichment was observed for Cd, Cu, Ni, Pb and Zn. This is not surprising for Cd, Cu, Ni, Pb and V since atmospheric dissolved inputs represent less than 1% of marine stocks. As expected from the comparison between inputs and stocks before rain, the marine dCo and dFe stocks were increased after dust deposition. However, the marine deltas within the ML for Co and Fe was 2 and 7 times higher than what could be provided from the atmospheric dissolved inputs. A lateral transport and cumulative effect of previous and surrounding wet deposition events (from 3 June) could explain this positive mismatch. Several removal processes occurring in the ocean, such as biological uptake (Morel et al., 2003; Noble et al., 2008), passive scavenging by adsorption onto particles (Wuttig et al., 2013, Bressac and Guieu., 2013, Mackey et al., 2015; Migon et al., 2020) or chemical processes as precipitation (Wagener et al., 2010, Ye et al., 2011) are known to decrease dissolved TM concentrations in the first 24 or 48 hours after atmospheric deposition. During the cruise, Bressac et al. (2021) show that dust deposition represented a significant input of dissolved Fe in the ML only on a timescale of hours, due to scavenging or precipitation processes. It is highly probable that these removal processes limited the cumulative effect of dTM inputs. A post-deposition dissolution of Fe and Mn in seawater was reported during dust seeding experiments simulating wet dust deposition in mesocosms over several hours or days (Wagener et al., 2008; Wuttig et al., 2013; Desboeufs et al., 2014). Mackey et al. (2015) show that in case of dry deposition, aerosol Co and Fe dissolution in seawater can be gradual and continue up to 7 days after contacting seawater. Considering the excess of TMs in marine stocks relative to rain inputs, our observations are consistent with the dissolution of Co and Fe in surface seawater following the first hours after wet dust deposition. Tovar-Sanchez et al., (2020) proposed that UV irradiation and the enrichment in organic matter in the SML could enhanced the dissolution processes and the diffusive transfer between SML and surface sea water. They estimated that the residence times ranged from 23 min. for pFe to 3.5 h for pCo in the SML after Rain FAST. From these timescales, the contribution of dissolution then diffusive process of dCo and dFe from SML to ML in the post-depositional dissolution processes could be considered. The increase of dissolved stocks suggested also that in the first hours after rain the dissolution processes were predominant on removal processes in the behaviour of dCo and dFe. Co and Fe being known to limit phytoplankton biomass, a biological uptake could be predominant if marine biota was limited for these elements. This was probably not the case here. The behaviour of Zn is more complicated to interpret since no enrichment was observed whereas the atmospheric dZn inputs represented around 12% of marine stocks. This unexpected behaviour could be explained by the predominant role of removal processes relative to post-depositional dissolution. The high solubility of Zn in Rain FAST (~86%), relative to solubility

values of Fe (8%) or Co (52%), suggests that all the soluble Zn was already dissolved in the rain inputs before contacting with seawater.

Finally, our results show that the studied atmospheric dust event was a net source of particulate TMs and dissolved Fe and Co for the ML at FAST. Even if the wet deposition delivered TMs already as soluble forms (Fig. 8), our results showed that the wet deposition constitutes only a source of some of dissolved TMs for surface waters. Due to various marine post-deposition processes, it is more complicated to observe the effect of wet deposition on dissolved stocks. The post-deposition dissolution of particulate rain inputs could represent an additional pathway of dissolved TM supply for the surface ocean, notably for low soluble TMs in wet deposition. Thus, the dissolved atmospheric inputs could be underestimate from the only measurements of atmospheric fluxes. On a timescale of hours, the Fe inventory was the most impacted by the dusty rain input, both in dissolved and particulate phases, confirming that the dust-rich rains are an external source of Fe to the surface Med Sea (Bonnet and Guieu, 2006, Bressac et al., 2021).

4.2.3. Comparison between TM wet atmospheric inputs and marine stocks in the western and central Mediterranean Sea

As discussed from dissolved TM stocks at FAST, high surface marine TM stocks masked any additional input for several TMs. However, the collected rains (FAST and ION) were originating from large rain systems covering more than 50 000 km^2 around the sampling zone and were typical of Mediterranean wet deposition. The wet deposition could have so occurred in any of the explored areas during the cruise. Here we further study the role of wet deposition by comparing atmospheric dissolved fluxes to marine dissolved stocks from TM profiles in the ML at all 13 marine stations, i.e. 22 ML samplings, throughout the whole cruise (Fig. 10). Exceptional intense dust deposition events have been recorded in the Mediterranean, reaching 20 g m^{-2} (Bonnet and Guieu, 2006). Sporadic and intense wet dust deposition higher than 1 g m^{-2} are observed in the spring in the western Mediterranean basin (e.g., Vincent et al., 2016). At the beginning of the cruise, an intense wet dust deposition event (not collected) occurred over the South of Sardinia and over the Tyrrhenian Sea with fluxes reaching about 9 g m^{-2} (Bressac et al., 2021). In order to take into account the effect of such intense event, we also estimated the atmospheric fluxes of dissolved TMs based on a 9 g m^{-2} wet dust deposition event using solubility values estimated from Rain FAST (Fig. 10). Fe, Mn and Pb solubility decreases with increasing dust load in Mediterranean rain samples (Theodosi et al., 2010), suggesting that this estimation is probably a maximum flux for

such deposition event. However, recent studies from aerosol collected in Atlantic Ocean showed that Co and Mn solubility was little affected by dust load at the difference of Fe (Baker et al., 2020). The impact of rain inputs on TM marine stocks is also controlled by MLD fluctuations which we ignored in this work by using a fixed ML depth at FAST and ION. As the variability of this MLD (7-21 m during the cruise, typical of Med thermal stratified period) could change the marine budgets by a factor of 3, we used the measured MLD (Van Wambeke et al., 2020) at each station for calculating the TM marine stocks.

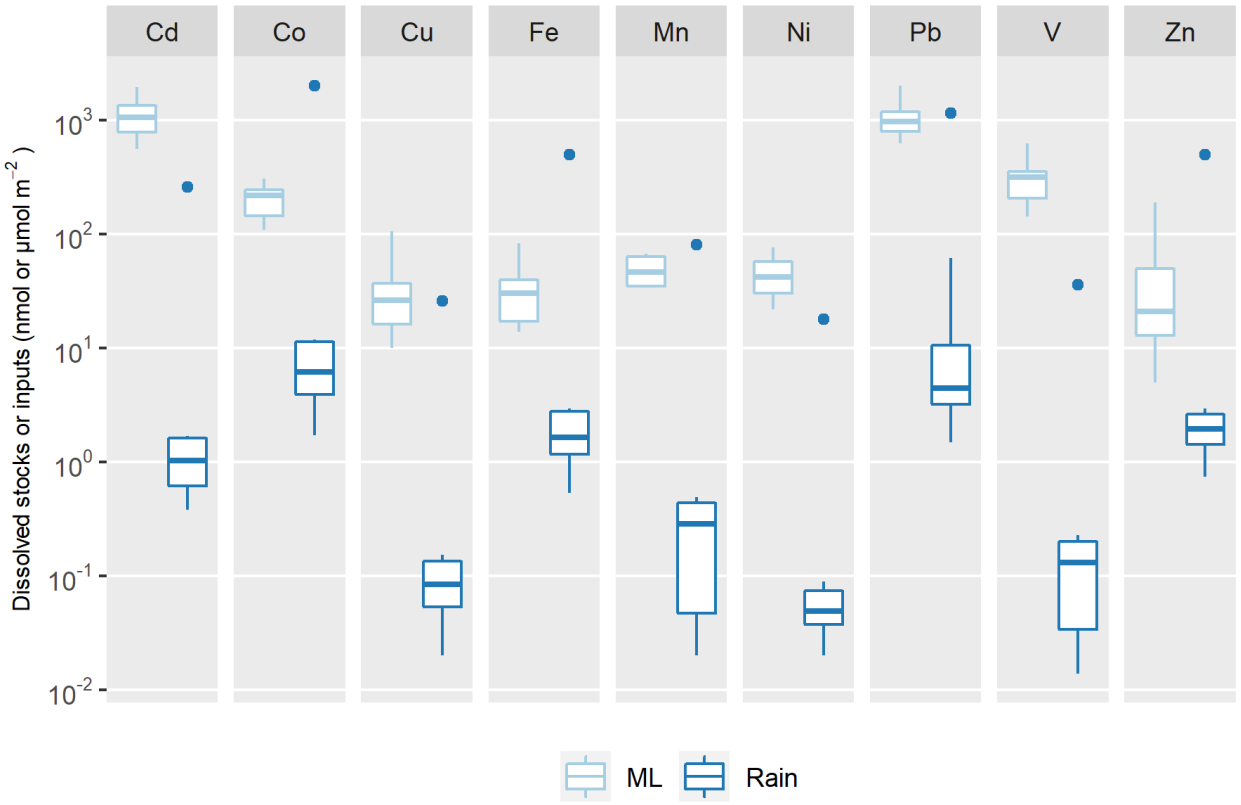

Figure 10: Comparison of marine stocks in the ML at all the stations occupied during the PEACETIME cruise (light blue boxes) with atmospheric deposition fluxes estimated (1) from ION and FAST rains (dark blue boxes) and (2) from an intense wet dust deposition event of 9 g m^{-2} (blue dots). Cd, Co and Pb stocks and fluxes are in nmol m^{-2}, and the other TMs in µmol m^{-2}. For Mn, marine stocks are derived from surface concentrations close to Corsica coasts (Wuttig et al., 2013: samples OUT at 0, 5 and 10 m) and in the Ionian Sea (Saager et al., 1993: Bannock basin at 0, 10, and 15 m), as no measurement is available from the PEACETIME cruise. Boxes and whiskers as in Fig. 4.

Applying to the whole transect, the atmospheric inputs, obtained from our rain composition, were at least 100-fold smaller than the dissolved stocks in the mixed layer, except for Co, Fe and Zn. The atmospheric inputs represented more than 30% of the dissolved Zn stocks and 10 to 18% for Fe.

For Co, the maximum atmospheric fluxes estimated during the cruise represented 5% of stocks. This significant input of dFe and dCo is in agreement with our field observations in the FAST ML. Here the comparison is based only on dissolved TMs in rain water, yet as discussed previously, the post-deposition deposition of atmospheric particles in the water column could further enrich the marine dissolved stocks for low soluble TMs, as Co, Fe, Mn, Ni, Pb or Ti. The surface seawater could be significantly affected by the deposition of these dissolved elements in the case of wet dust deposition. In the case of the intense dust deposition event, the dissolved inputs are of the same order of magnitude as marine stocks for Co, Fe, Mn, Pb and Zn. The enrichment in dFe and dMn was previously observed by Wuttig et al. (2013) after artificial dust seeding in large mesocosms (simulating a wet deposition event of 10 g m^{-2}). The marine TM concentrations measured during the cruise being typical of Mediterranean surface seawater concentrations, we can conclude that wet deposition events were an external supply of dissolved Fe, Co and Zn for the Med Sea, and more generally for all TMs in case of intense wet dust deposition, during the period of thermal stratification.

5. Conclusions

This study provides both the dynamic properties and chemical characterization of two rain events collected in the open Mediterranean Sea, concurrently with TM marine stocks in surface seawater. Our results are the only recent report of TM concentrations, EFs and fractional solubility values in rain samples collected in the remote Med Sea. By highlighting the discrepancy between TM concentrations with the previous offshore and coastal rain studies, this work demonstrates the need to provide a new and recent database on TM composition in Mediterranean rains in order to estimate the role of atmospheric TM deposition. We have shown the representativeness of Rain FAST as typical of Saharan dust wet deposition in its chemical composition as well in its magnitude and extent, whereas Rain ION is more-typical of an anthropogenic background rain for the remote Med Sea. On this basis, we suggest using the chemical composition of PEACETIME rains as a new reference for studies of TMs on wet deposition in the Med Sea. This study was focused on wet deposition, yet dry deposition is also an important source of TMs to surface waters in Med Sea (Theodosi et al., 2010). As the wet deposition fluxes decreased since the 90's due to mitigation, it is highly probable that the dry deposition fluxes were also changed. Further measurements of dry deposition in open Med Sea are needed in order to estimate its contribution in TM atmospheric inputs.

Since atmospheric TMs have been identified as critical oligo-nutrients for the marine biosphere, it is important to study the response of the receiving waters to atmospheric inputs. This study is the first to provide *in situ* evidence that atmospheric wet deposition constitutes a significant external source for some of these elements to surface stratified Mediterranean seawater. We recommend that the original approach developed here is used in other parts of the world where atmospheric wet deposition is thought to impact the marine biosphere, such as in HNLC (High Nutrient, Low Chlorophyll) regions.

Data availability. Guieu et al., Biogeochemical dataset collected during the PEACETIME cruise. SEANOE. https://doi.org/10.17882/75747 (2020). Atmospheric Data are accessible on http://www.obs-vlfr.fr/proof/php/PEACETIME/peacetime.php.

Author contributions. KD and FF designed the study and wrote the manuscript; FF, ST, JFD, Ch.G made the on-board atmospheric measurements and sampling during the cruise; FF, ST and JD analysed the rain samples; MB, ATS, and ARR made the marine TMs sampling and analyses; PF was the reference scientist of PEGASUS, AF and FM managed all the technical preparation of atmospheric samplings, PC analysed the lidar data; KD, FD and Ce.G designed the cruise strategy; KD and Ce.G coordinated the PEACETIME project, FD coordinated the ChArMEx funding request, and near-real time and forecast survey of atmospheric conditions during the cruise; all the authors commented on the manuscript and contributed to its improvement.

Competing interests. The authors declare that they have no conflict of interest.

Special issue statement. This article is part of the special issue "Atmospheric deposition in the low-nutrient–low-chlorophyll (LNLC) ocean: effects on marine life today and in the future (ACP/BG inter- journal SI)". It is not associated with a conference.

Acknowledgements. The authors wish to thank Thierry Alix the captain of the R/V *Pourquoi Pas ?* as well as the whole crew and technical staff for their involvement in the scientific operation. We gratefully thank Thibaut Wagener for his involvement in the trace-metals clean marine sampling and Mickaël Tharaud for the HR-ICP-MS analysis. We thank the Leosphere Technical support team and especially Alexandre Menard for their remote assistance with LIDAR repair under difficult off-shore conditions. Hélène Ferré and the AERIS/SEDOO service are acknowledged for real-time collection during the cruise of maps from operational satellites and forecast models used in this study, with appreciated contributions of EUMETSAT and AERIS/ICARE for MSG/SEVIRI products. EUMETNET is acknowledged for providing the pan-European weather radar composite images through its OPERA programme. We acknowledge the US National Oceanic and Atmospheric Administration (NOAA) Air Resources Laboratory (ARL) for the provision of the HYSPLIT (HYbrid Single-Particle Lagrangian Integrated Trajectory) model via NOAA

ARL READY website (http://ready.arl.noaa.gov) used in this publication. This study is a contribution to the PEACETIME project (http://peacetime-project.org; last accessed 05/04/2021), a joint initiative of the MERMEX and ChArMEx programmes supported by CNRS-INSU, IFREMER, CEA and Météo-France as part of the decadal meta-programme MISTRALS coordinated by CNRS-INSU. PEACETIME was endorsed as a process study by GEOTRACES and is also a contribution to IMBER and SOLAS international programs. The authors gratefully thank Rachel Shelley and the anonymous reviewer for their useful comments and critiques which have contributed to improve the manuscript.

References

Achterberg, E. P., Braungardt, C. B., Sandford, R. C. and Worsfold, P. J.: UV digestion of seawater samples prior to the determination of copper using flow injection with chemiluminescence detection, Anal. Chim. Acta, 440, 27–36, https://doi.org/10.1016/S0003-2670(01)00824-8, 2001.

Al-Momani, I. F., Aygun, S., and Tuncel, G.: Wet Deposition of Major Ions and TMs in the Eastern Mediterranean Basin, J. Geophys. Res. (Atmos.), 103, 8287–8299, https://doi.org/10.1029/97JD03130, 1998.

Amato, F., Alastuey, A., Karanasiou, A., Lucarelli, F., Nava, S., Calzolai, G., Severi, M., Becagli, S., Gianelle, V. L., Colombi, C., Alves, C., Custódio, D., Nunes, T., Cerqueira, M., Pio, C., Eleftheriadis, K., Diapouli, E., Reche, C., Minguillón, M. C., Manousakas, M.-I., Maggos, T., Vratolis, S., Harrison, R. M., and Querol, X.: AIRUSE-LIFE+: a harmonized PM speciation and source apportionment in five southern European cities, Atmos. Chem. Phys., 16, 3289–3309, https://doi.org/10.5194/acp-16-3289-2016, 2016.

Annett, A. L., Lapi, S., Ruth, T. J., and Maldonado, M. T.: The effects of Cu and Fe availability on the growth and Cu:C ratios of marine diatoms, Limnol. Oceanogr., 53, 2451–2461, https://doi.org/10.4319/lo.2008.53.6.2451, 2008.

Avila, A., Queralt‐Mitjans, I., and Alarcón, M.: Mineralogical composition of African dust delivered by red rains over northeastern Spain, J. Geophys. Res. Atmos., 102, 21977–21996, https://doi.org/10.1029/97JD00485, 1997.

Baconnais, I., Rouxel, O., Dulaquais, G., and Boye, M.: Determination of the copper isotope composition of seawater revisited: A case study from the Mediterranean Sea, Chem. Geol., 511, 465–480, https://doi.org/10.1016/j.chemgeo.2018.09.009, 2019.

Baker, A. R., Adams, C., Bell, T. G., Jickells, T. D., and Ganzeveld, L., Estimation of atmospheric nutrient inputs to the Atlantic Ocean from 50°N to 50°S based on large-scale field sampling: Iron and other dust-associated elements, Global Biogeochem. Cycles, 27, 755– 767, doi:10.1002/gbc.20062, 2013.

Baker, A. R., Li, M., & Chance, R., Trace metal fractional solubility in size-segregated aerosols from the tropical eastern Atlantic Ocean. Global Biogeochemical Cycles, 34, e2019GB006510. https://doi.org/10.1029/2019GB006510, 2020.

Becagli, S., Anello, F., Bommarito, C., Cassola, F., Calzolai, G., Iorio, T. D., Sarra, A. D., Gómez-Amo, J. L., Lucarelli, F., Marconi, M., and Meloni, D.: Constraining the ship contribution to the aerosol of the central Mediterranean, Atmosp. Chem. Phys., 17, 2067–2084, , https://doi.org/10.5194/acp-17-2067-2017, 2017.

Bergametti, G., Gomes, L., Remoudaki, E., Desbois, M., Martin, D., and Buat-Ménard, P.: Present transport and deposition patterns of African dusts to the North-Western Mediterranean, in Paleoclimatology and Paleometeorology: Modern and past patterns of global atmospheric transport, Leinen, M., and Sarnthein, M., Eds., Springer, Dordrecht, NATO ASI Ser. C, 282, 227–252, https://doi.org/10.1007/978-94-009-0995-3_9, 1989.

Béthoux, J.P., Courau, P., Nicolas, E., and Ruiz-Pino, D.: Trace metal pollution in the Mediterranean Sea, Oceanol. Acta 13, 481–488, https://archimer.ifremer.fr/doc/00103/21418/ (last accessed 03 July 2021), 1990.

Bonnet, S. and Guieu, C.: Dissolution of atmospheric iron in seawater, Geophys. Res. Lett., 31, L03303, https://doi.org/10.1029/2003GL018423, 2004.

Bonnet, S., and Guieu, C.: Atmospheric forcing on the annual iron cycle in the western Mediterranean Sea: A 1-year survey, J. Geophys. Res., 111, C09010, https://doi.org/10.1029/2005JC003213, 2006.

Bove, M. C., Brotto, P., Calzolai, G., Cassola, F., Cavalli, F., Fermo, P., Hjorth, J., Massabò, D., Nava, S., Piazzalunga, A., and Schembari, C.: PM_{10} source apportionment applying PMF and chemical tracer analysis to ship-borne measurements in the Western Mediterranean, Atmos. Environ., 125, 140–151, https://doi.org/10.1016/j.atmosenv.2015.11.009, 2016.

Bressac, M., and Guieu, C.: Post-depositional processes: What really happens to new atmospheric iron in the ocean's surface?, *Global Biogeochem. Cycles*, 27, 859– 870, doi:10.1002/gbc.20076, 2013

Bressac, M., Wagener, T., Leblond, N., Tovar-Sánchez, A., Ridame, C., Taillandier, V., Albani, S., Guasco, S., Dufour, A., Jacquet, S. H. M., Dulac, F., Desboeufs, K., and Guieu, C.: Subsurface iron accumulation and rapid aluminum removal in the Mediterranean following African dust deposition, Biogeosciences, 18, 6435–6453, https://doi.org/10.5194/bg-18-6435-2021, 2021.

Bruland, K. W., Franks, R. P., Knauer, G. A. and Martin, J. H.: Sampling and analytical methods for the determination of copper, cadmium, zinc, and nickel at the nanogram per liter level in sea water, Anal. Chim. Acta, 105, 233–245, https://doi.org/10.1016/S0003-2670(01)83754-5, 1979.

Buat-Ménard, P., and Chesselet, R.: Variable influence of the atmospheric flux on the trace metal chemistry of oceanic suspended matter, Earth Planet. Sci. Lett., 42, 399–411, https://doi.org/10.1016/0012-821X(79)90049-9, 1979.

Buat-Ménard, P.: Particle geochemistry in the atmosphere and oceans, In: Air-Sea Exchange of Gases and Particles, Liss P.S., Slinn W.G.N. Editors, NATO ASI Series C, 108, 455–532, Springer, Dordrecht, https://doi.org/10.1007/978-94-009-7169-1_8, 1983..

Chance, R., Jickells, T. D. and Baker, A.R.: Atmospheric Trace Metal Concentrations, Solubility and Deposition Fluxes in Remote Marine Air over the South-East Atlantic, Mar. Chem., 177, 45–56, https://doi.org/10.1016/j.marchem.2015.06.028, 2015.

Chazette, P., Flamant, C., Totems, J., Gaetani, M., Smith, G., Baron, A., Landsheere, X., Desboeufs, K., Doussin, J.-F., and Formenti, P.: Evidence of the complexity of aerosol transport in the lower troposphere on the Namibian coast during AEROCLO-sA, Atmos. Chem. Phys., 19, 14979–15005, https://doi.org/10.5194/acp-19-14979-2019, 2019.

Chazette, P., Totems, J., Ancellet, G., Pelon, J., and Sicard, M.: Temporal consistency of lidar observations during aerosol transport events in the framework of the ChArMEx/ADRIMED campaign at Minorca in June 2013, Atmos. Chem. Phys., 16, 2863–2875, https://doi.org/10.5194/acp-16-2863-2016, 2016.

Chester, R., Nimmo, M., Corcoran, P. A.: Rain water-aerosol trace metal relationships at Cap Ferrat: a coastal site in the Western Mediterranean, Mar. Chem., 58, 293–312, https://doi.org/10.1016/S0304-4203(97)00056-X, 1997.

Desboeufs, K., Losno, R., Vimeux, F., Cholbi, S.: the pH-dependent dissolution of wind transported Saharan dust. J. Geophys. Res., 104, 21287–21299, https://doi.org/10.1029/1999JD900236, 1999.

Desboeufs, K. V., Sofikitis, A., Losno, R., Colin, J. L., and Ausset, P.: Dissolution and solubility of trace metals from natural and anthropogenic aerosol particulate matter, Chemosphere, 58, 195–203, https://doi.org/10.1016/j.chemosphere.2004.02.025, 2005.

Desboeufs. K., Leblond, N., Wagener, T., Bon Nguyen, E., Guieu, C.: Chemical fate and settling of mineral dust in surface seawater after atmospheric deposition observed from dust seeding experiments in large mesocosms, Biogeosciences, 11, 5581–5594, https://doi.org/10.5194/bg-11-5581-2014, 2014.

Desboeufs, K., Bon Nguyen, E., Chevaillier, S., Triquet, S., and Dulac, F.: Fluxes and sources of nutrient and trace metal atmospheric deposition in the northwestern Mediterranean, Atmos. Chem. Phys., 18, 14477–14492, https://doi.org/10.5194/acp-18-14477-2018, 2018.

Desboeufs, K.: Trace metals and contaminants deposition, in Atmospheric Chemistry in the Mediterranean – Vol. 2, From Pollutant Sources to Impacts, edited by Dulac, F., Sauvage, S., and Hamonou, E., Springer, Cham, Switzerland, in press, 2021.

Duce, R. A., P. S. Liss, J. T. Merrill, E. L. Atlas, P. Buat-Menard, B. B. Hicks, J. M. Miller, J. M. Prospero, R. Arimoto, T. M. Church, W. Ellis, J. N. Galloway, L. Hansen, T. D. Jickells, A. H. Knap, K. H. Reinhardt, B. Schneider, A. Soudine, J. J. Tokos, S. Tsunogai, R. Wollast, M. Zhou, The atmospheric input of trace species to the world ocean, Global Biogeochem. Cycles, 5(3), 193– 259, doi:10.1029/91GB01778, 1991.

Dulac, F.: Dynamique du transport et des retombées d'aérosols métalliques en Méditerranée occidentale, PhD Dissertation, Univ. Paris 7, 241 pp., 1986.

Dulaquais, G., H. Planquette, S. L'Helguen, M. J. A. Rijkenberg, and M. Boye, The biogeochemistry of cobalt in the Mediterranean Sea, Global Biogeochem. Cycles, 31, 377–399, doi:10.1002/2016GB005478, 2017.

Formenti, P., D'Anna, B., Flamant, C., Mallet, M., Piketh, S. J., Schepanski, K., Waquet, F., Auriol, F., Brogniez, G., Burnet, F., Chaboureau, J., Chauvigné, A., Chazette, P., Denjean, C., Desboeufs, K., Doussin, J., Elguindi, N., Feuerstein, S., Gaetani, M., Giorio, C., Klopper, D., Mallet, M. D., Nabat, P., Monod, A., Solmon, F., Namwoonde, A., Chikwililwa, C., Mushi, R., Welton, E. J., and Holben, B.: The Aerosols, Radiation and Clouds in southern Africa field campaign in Namibia: Overview, illustrative observations, and way forward, Bull. Am.Meteorol. Soc., 100, 1277–1298, https://doi.org/10.1175/BAMS-D-17-0278.1, 2019.

Frau, F., Caboi, R., and Cristini, A.: The impact of Saharan dust on TMs solubility in rainwater in Sardinia, Italy, In: The Impact of Desert Dust Across the Mediterranean, S. Guerzoni, and R. Chester (Eds.), Springer, Dordrecht, Environ. Sci. Technol. Library, 11, 285–290, https://doi.org/10.1007/978-94-017-3354-0_28, 1996.

Fu, Y.F., Desboeufs, K., Vincent, J., Bon Nguyen, E., Laurent, B., Losno, R., and Dulac, F.: Estimating chemical composition of atmospheric deposition fluxes from mineral insoluble particles deposition collected in the western Mediterranean region, Atmos. Meas. Tech., 10, 4389–4401, https://doi.org/10.5194/amt-10-4389-2017, 2017.

Fu, F., Desboeufs, K., Triquet, S., Doussin J.-F., Giorio C., Chevaillier S., Feron A., Formenti, F., Maisonneuve F., Riffautl, V.: Aerosol characterisation and quantification of trace element atmospheric dry deposition fluxes in remote Mediterranean Sea during PEACETIME cruise, Atmos. Chem. Phys., in prep.

Gallisai, R., Peters, F., Volpe, G., Basart., and Baldasano J. M.: Saharan Dust deposition may affect phytoplankton growth in the Mediterranean S. Sea at ecological time scales, PLoS One, 9, e110762, https://doi.org/10.1371/journal.pone.0110762, 2014.

Guerzoni. S, E Molinaroli, P Rossini, G Rampazzo, G Quarantotto, S Cristini.: Role of desert aerosol in metal fluxes in the Mediterranean area, Chemosphere, 39, 229–246, https://doi.org/10.1016/S0045-6535(99)00105-8, 1999b.

Guieu, C., and Ridame, C., Impact of atmospheric deposition on marine chemistry and biogeochemistry, in: Atmospheric Chemistry in the Mediterranean - Vol. 2, From Air Pollutant Sources to Impacts, edited by Dulac, F., Sauvage, S., and Hamonou, E., Springer, Cham, Switzerland, in press, 2021.

Guieu, C., Chester, R., Nimmo, M., Martin, J. M., Guerzoni, S., Nicolas, E., Mateu, J., and Keyse, S.: Atmospheric input of dissolved and particulate metals to the North Western Mediterranean, Deep Sea Res. II, 44, 655–674, https://doi.org/10.1016/S0967-0645(97)88508-6, 1997.

Guieu, C., Loye-Pilot, M. D., Ridame, C., and Thomas, C.: Chemical Characterization of the Saharan dust endmember: Some biogeochemical implications for the Western Mediterranean Sea, J. Geophys. Res., 107, 4258, https://doi.org/10.1029/2001JD000582, 2002.

Guieu, C., Bonnet, S., Wagener, T., and Loÿe-Pilot, M.-D.: Biomass burning as a source of dissolved iron to the open ocean?, Geophys. Res. Lett., 32, L19608, https://doi.org/10.1029/2005GL022962, 2005.

Guieu. C, M.-D. Loÿe-Pilot, L. Benyahya, A. Dufour.: Spatial variability of atmospheric fluxes of metals (Al, Fe, Cd, Zn and Pb) and phosphorus over the whole Mediterranean from a one-year monitoring experiment: Biogeochemical implications, Mar. Chem., 120, 164–178, https://doi.org/10.1016/j.marchem.2009.02.004, 2010.

Guieu, C., D'Ortenzio, F., Dulac, F., Taillandier, V., Doglioli, A., Petrenko, A., Barrillon, S., Mallet, M., Nabat, P., and Desboeufs, K.: Introduction: Process studies at the air-sea interface after atmospheric deposition in the Mediterranean Sea – objectives and strategy of the PEACETIME oceanographic campaign (May–June 2017), Biogeosciences, 17, 5563–5585, https://doi.org/10.5194/bg-17-5563-2020, 2020.

Hardy, J. T.:. The sea surface microlayer: biology, chemistry and anthropogenic enrichment, Prog. Oceanogr., 11, 307–328, https://doi.org/10.1016/0079-6611(82)90001-5, 1982.

Heimbürger, L. E., Migon, C., Dufour, A., Chiffoleau, J. F., and Cossa, D.: Trace metal concentrations in the North-western Mediterranean atmospheric aerosol between 1986 and 2008: Seasonal patterns and decadal trends, Sci. Total Environ., 408, 2629–2638, https://doi.org/10.1016/j.scitotenv.2010.02.042, 2010.

Heimburger, A., Losno, R., Triquet, S., Dulac F., and Mahowald, N. M.: Direct measurements of atmospheric iron, cobalt and aluminium-derived dust deposition at Kerguelen Islands, Global Biogeochem. Cycles, 26, GB4016, https://doi.org/10.1029/2012GB004301, 2012.

Heimburger, A., Losno, R., and Triquet, S.: Solubility of iron and other trace elements in rainwater collected on the Kerguelen Islands (South Indian Ocean), Biogeosciences, 10, 6617–6628, https://doi.org/10.5194/bg-10-6617-2013, 2013.

Hersbach, H., Bell, B., Berrisford, P., Biavati, G., Horányi, A., Muñoz Sabater, J., Nicolas, J., Peubey, C., Radu, R., Rozum, I., Schepers, D., Simmons, A., Soci, C., Dee, D., Thépaut, J-N.: ERA5 hourly data on single levels from 1979 to present, Copernicus Climate Change Service (C3S) Climate Data Store (CDS), https://doi.org/10.24381/cds.adbb2d47, 2018.

Herut, B., Krom, M. D., Pan, G., and Mortimer, R.: Atmospheric input of nitrogen and phosphorus to the Southeast Mediterranean: Sources, fluxes, and possible impact, Limnol. Oceanogr., 44, 1683–1692, https://doi.org/10.4319/lo.1999.44.7.1683, 1999.

Hydes, D.J., and Liss, P.S.: Fluorimetric method for the determination of low concentrations of dissolved aluminium in natural waters, Analyst, 101, 922–931, 1976.

GEOTRACES Intermediate Data Product Group, The GEOTRACES Intermediate Data Product 2021 (IDP2021). NERC EDS British Oceanographic Data Centre NOC. doi:10.5285/cf2d9ba9-d51d-3b7c-e053-8486abc0f5fd, 2021.

Gonzalez, L., and Briottet, X.: North Africa and Saudi Arabia day/night sandstorm survey (NASCube). Remote Sens., 9, 896, https://doi.org/10.3390/rs9090896, 2017.

Izquierdo, R., Benítez-Nelson, C. R., Masqué, P., Castillo, S., Alastuey, A., Castillo, S., Alastuey, A., and Avila, A.: Atmospheric phosphorus deposition in a near-coastal rural site in the NE Iberian Peninsula and its role in marine productivity, Atmos. Environ., 49, 361–370, https://doi.org/10.1016/j.atmosenv.2011.11.007, 2012.

Izquieta-Rojano, S., García-Gomez, H., Aguillaume, L., Santamaría, J. M., Tang, Y. S., Santamaría, C., Valiño, F., Lasheras, E., Alonso, R., Àvila, A., Cape, J. N., and Elustondo, D.: Throughfall and bulk deposition of dissolved organic nitrogen to holm oak forests in the Iberian Peninsula: flux estimation and identification of potential sources, Environ. Pollut., 210, 104–112, https://doi.org/10.1016/j.envpol.2015.12.002, 2016.

Jickells TD, Baker AR, Chance R., Atmospheric transport of trace elements and nutrients to the oceans. Phil. Trans. R. Soc. A 374: 20150286, http://dx.doi.org/10.1098/rsta.2015.0286, 2016

Jordi, A., Basterretxea, G., Tovar-Sánchez, A., Alastuey, A. and Querol, X.: Copper aerosols inhibit phytoplankton growth in the Mediterranean Sea, Proc. Nat. Acad. Sci., 109, 21246–21249, https://doi.org/10.1073/pnas.1207567110, 2012.

Kanakidou, M., Mihalopoulos, N., Kindap, T., Im, U., Vrekoussis, M., Gerasopoulos, E., Dermitzaki, E., Unal, A., Koçak, M., Markakis, K., Melas, D., Kouvarakis, G., Youssef, A. F., Richter, A., Hatzianastassiou, N., Hilboll, A., Ebojie, F., Wittrock, F., von Savigny, C., Burrows, J. P., Ladstaetter-Weissenmayer, A., and Moubasher, H.: Megacities as hot spots of air pollution in the East Mediterranean, Atmos. Environ., 45, 1223–1235, https://doi.org/10.1016/j.atmosenv.2010.11.048, 2011.

Kanellopoulou, E. A.: Determination of heavy metals in wet deposition of Athens, Global NEST J., 3, 45–50, https://doi.org/10.30955/gnj.000181, 2001.

Longo, A. F., Ingall, E. D., Diaz, J. M., Oakes, M., King, L. E., Nenes, A., Mihalopoulos, N., Violaki, K., Avila, A., Benitez-Nelson, C. R., Brandes, J., McNulty, I., and Vine, D. J.: P-NEXFS analysis of aerosol phosphorus delivered to the Mediterranean Sea, Geophys. Res. Lett., 41, 4043–4049, https://doi.org/10.1002/2014GL060555, 2014.

Losno, R.: Chimie d'éléments minéraux en traces dans les pluies méditerranéennes, Ph.D. thesis, Univ. Paris-Diderot de Paris 7, https://tel.archives-ouvertes.fr/tel-00814327/document (last accessed 4 July 2021), 1989.

Loÿe-Pilot, M.-D., and Martin, J. M.: Saharan dust input to the western Mediterranean: an eleven years record in Corsica, , In: The Impact of Desert Dust Across the Mediterranean, Guerzoni, S., Chester, R. (Eds.), Springer, Dordrecht, Environ. Sci. Technol. Library, 11, 191–199, https://doi.org/10.1007/978-94-017-3354-0_18, 1996.

Mackey, K. R. M., Buck, K. N., Casey, J. R., Cid, A., Lomas, M. W., Sohrin, Y., and Paytan, A.: Phytoplankton Responses to Atmospheric Metal Deposition in the Coastal and Open-Ocean Sargasso Sea, Front. Microbiol., 3, 359, https://doi.org/10.3389/fmicb.2012.00359, 2012.

Mallet, M. D., D'Anna, B., Même, A., Bove, M. C., Cassola, F., Pace, G., Desboeufs, K., Di Biagio, C., Doussin, J.-F., Maille, M., Massabò, D., Sciare, J., Zapf, P., di Sarra, A. G., and Formenti, P.: Summertime surface PM_1 aerosol composition and size by source region at the Lampedusa island in the central Mediterranean Sea, Atmos. Chem. Phys., 19, 11123–11142, https://doi.org/10.5194/acp-19-11123-2019, 2019.

Markaki, Z., Loëe-Pilot, M. D., Violaki, K., Benyahya, L., and Mihalopoulos, N.: Variability of atmospheric deposition of dis- solved nitrogen and phosphorus in the Mediterranean and possible link to the anomalous seawater N/P ratio, Mar. Chem., 120, 187–194, https://doi.org/10.1016/j.marchem.2008.10.005, 2010.

Migon, C., Robin, T., Dufour, A., and Gentili, B.: Decrease of lead concentrations in the Western Mediterranean atmosphere during the last 20 years, Atmos. Environ., 42, 815–821, https://doi.org/10.1016/j.atmosenv.2007.10.078, 2008.

Migon, C., Heimbürger-Boavida, L.-E., Dufour, A., Chiffoleau, J.-F., and Cossa, D.: Temporal variability of dissolved trace metals at the DYFAMED time-series station, Northwestern Mediterranean, Mar. Chem., 225, 103846, https://doi.org/10.1016/j.marchem.2020.103846, 2020.

Millero, F.J., Chemical Oceanography (4th ed.). CRC Press. https://doi.org/10.1201/b14753, 2013.

Milne, A., Landing, W., Bizimis, M., and Morton, P.: Determination of Mn, Fe, Co, Ni, Cu, Zn, Cd and Pb in seawater using high resolution magnetic sector inductively coupled mass spectrometry (HR-ICP-MS), Analytica Chimica Acta, 665, 200–207, https://doi.org/10.1016/j.aca.2010.03.027, 2010.

Morel, F. M. M., Hudson, R. J. M., and Price, N. M: Limitation of productivity by trace metals in the sea, Limnol. Oceanogr, 36, 1742–1755, https://doi.org/10.4319/lo.1991.36.8.1742, 1991.

Morel, F. M., Milligan, A. J., & Saito, M. A. Marine bioinorganic chemistry: the role of trace metals in the oceanic cycles of major nutrients. Treatise on geochemistry, 6, 625, https://doi.org/10.1016/B0-08-043751-6/06108-9, 2003.

Morin, E., Krajeski, W. F., Goorich, D. C., Gao, X., and Sorooshian, S.: Estimating rainfall intensities from weather radar data: The scale-dependency problem, J. Hydrometeorol., 4, 782–797, https://doi.org/10.1175/1525-7541(2003)004<0782:ERIFWR>2.0.CO;2, 2003.

Morley, N. H., Burton, J. D., Tankere, S. P. C., and Martin, J.-M.: Distribution and behaviour of some dissolved trace metals in the western Mediterranean Sea, Deep Sea Res. II, 44, 675–691, https://doi.org/10.1016/S0967-0645(96)00098-7, 1997.

Nehir, M., and Koçak, M.: Atmospheric water-soluble organic nitrogen (WSON) in the eastern Mediterranean: origin and ramifications regarding marine productivity, Atmos. Chem. Phys., 18, 3603–3618, https://doi.org/10.5194/acp-18-3603-2018, 2018.

Ochoa-Hueso, R., Allen, E. B., Branquinho, C., Cruz, C., Dias, T., Fenn, M. E., Manrique, E., Perez-Corona, M. E., Sheppard, L. J., and Stock, W. D.: Nitrogen deposition effects on Mediterranean-type ecosystems: an ecological assessment, Environ. Pollut., 159, 2265–2279, https://doi.org/10.1016/j.envpol.2010.12.019, 2011.

OSPAR Commission: Atmospheric deposition of selected heavy metals and persistent organic pollutants to the OSPAR maritime area (1990 – 2005). Publication 375/2008, 2008.Özsoy, T., and Örnektekin, S.: TMs in Urban and Suburban Rainfall, Mersin, Northeastern Mediterranean, Atmos. Res., 94, 203–219, https://doi.org/10.1016/j.atmosres.2009.05.017, 2009.Pacyna, E. G., Pacyna, J. M., Fudala, J., Strzelecka-Jastrzab, E., Hlawiczka, S., Panasiuk, D., Nitter, S., Pregger, T., Pfeiffer, H., and Friedrich, R.: Current and future emissions of selected heavy metals to the atmosphere from anthropogenic sources in Europe, Atmos. Environ., 41, 8557–8566, https://doi.org/10.1016/j.atmosenv.2007.07.040, 2007.

Paris, R., and Desboeufs, K. V.: Effect of atmospheric organic complexation on iron-bearing dust solubility, Atmos. Chem. Phys., 13, 4895–4905, https://doi.org/10.5194/acp-13-4895-2013, 2013.

Pinedo-González, P., Joshua West, A., Tovar-Sánchez, A., Duarte, C. M., Marañón, E., Cermeño, P., González, N., Sobrino, C., Huete-Ortega, M., Fernández, A., López-Sandoval, D. C., Vidal, M., Blasco, D., Estrada, M., and Sañudo-Wilhelmy, S. A.: Surface distribution of dissolved trace metals in the oligotrophic ocean and their influence on phytoplankton biomass and productivity, Global. Biogeochem. Cycles, 29, 1763–1781, https://doi.org/10.1002/2015GB005149, 2015.

Powell, C. F., Baker, A. R., Jickells, T. D., Bange, H. W., Chance, R. J., and Yodle, C.: Estimation of the atmospheric flux of nutrients and trace metals to the eastern tropical North Atlantic Ocean, J. Atmos. Sci., 72, 4029–4045, https://doi.org/10.1175/JAS-D-15-0011.1, 2015.

Pulido-Villena, E., Rérolle, V., and Guieu, C.: Transient fertilizing effect of dust in P-deficient LNLC surface ocean, Geophys. Res. Lett., 37, L01603, https://doi.org/10.1029/2009GL041415, 2010.

Pulido-Villena, E., Desboeufs, K., Djaoudi, K., Van Wambeke, F., Barrillon, S., Doglioli, A., Petrenko, A., Taillandier, V., Fu, F., Gaillard, T., Guasco, S., Nunige, S., Triquet, S., and Guieu, C.: Phosphorus cycling in the upper waters of the Mediterranean Sea (PEACETIME cruise): relative contribution of external and internal sources, Biogeosciences, 18, 5871–5889, https://doi.org/10.5194/bg-18-5871-2021, 2021.

Rahn, K. A.: The Chemical Composition of the Atmospheric Aerosol, Tech. Rept., Graduate School of Oceanography, Univ. Rhode Island, Kingston, RI, 265 pp., https://books.google.fr/books?id=q-dOAQAAMAAJ (last accessed 04 July 2021), 1976.

Raut, J.-C., and Chazette, P.: Assessment of vertically-resolved PM10 from mobile lidar observations, Atmos. Chem. Phys., 9, 8617-8638, https://doi.org/10.5194/acp-9-8617-2009, 2009.

Richon, C., Dutay, J.-C., Dulac, F., Wang, R., and Balkanski, Y.: Modeling the biogeochemical impact of atmospheric phosphate deposition from desert dust and combustion sources to the Mediterranean Sea, Biogeosciences, 15, 2499–2524, https://doi.org/10.5194/bg-15-2499-2018, 2018a.

Richon, C., Dutay, J.C., Dulac, F., Wang, R., Balkanski, Y., Nabat, P., Aumont, O., Desboeufs, K., Laurent, B., Guieu, C., and Raimbault, P.: Modeling the impacts of atmospheric deposition of nitrogen and desert dust-derived phosphorus on nutrients and biological budgets of the Mediterranean Sea, Prog. Oceanogr., 163, 21–39, https://doi.org/10.1016/j.pocean.2017.04.009, 2018b.

Ridame, C., Le Moal, M., Guieu, C., Ternon, E., Biegala, I. C., L'Helguen, S., and Pujo-Pay, M.: Nutrient control of N2 fixation in the oligotrophic Mediterranean Sea and the impact of Saharan dust events, Biogeosciences, 8, 2773–2783, https://doi.org/10.5194/bg-8-2773-2011, 2011.

Royer, P., Chazette, P., Lardier, M., and Sauvage, L.: Aerosol content survey by mini N2-Raman lidar: Application to local and long-range transport aerosols, Atmos. Environ., 45, 7487–7495, https://doi.org/10.1016/j.atmosenv.2010.11.001, 2011.

Rudnick, R. L., and Gao, S.: Composition of the Continental Crust. In: Treatise on Geochemistry, Holland, H. D., and Turekian, K. K. (Editors), Elsevier, Amsterdam. 3, 1–64, 2003.

Saager, P. M., Schijf, J., and de Baar, H. J. W.: Trace-metal distributions in seawater and anoxic brines in the eastern Mediterranean Sea, Geochim. Cosmochim. Acta, 57, 1419–1432, https://doi.org/10.1016/0016-7037(93)90003-F, 1993.

Sandroni, V., and Migon, C.: Atmospheric deposition of metallic pollutants over the Ligurian Sea: labile and residual inputs, Chemosphere, 47, 753–764, https://doi.org/10.1016/s0045-6535(01)00337-x, 2002.

Saltikoff, E., Haase, G., Delobbe, L., Gaussiat, N., Martet, M., Idziorek, D., Leijnse, H., Novák, P., Lukach, M., and Stephan, K.: OPERA the Radar Project, Atmosphere, 10, 320, https://doi.org/10.3390/atmos10060320, 2019.

Sciare, J., Bardouki, H., Moulin, C., and Mihalopoulos, N.: Aerosol sources and their contribution to the chemical composition of aerosols in the Eastern Mediterranean Sea during summertime, Atmos. Chem. Phys., 3, 291–302, https://doi.org/10.5194/acp-3-291-2003, 2003.

Sedwick, P. N., Sholkovitz, E. R., and Church, T. M.: Impact of anthropogenic combustion emissions on the fractional solubility of aerosol iron: Evidence from the Sargasso Sea, Geochem. Geophys. Geosyst., 8, Q10Q06, doi:10.1029/2007GC001586.Sherrell, R. M. and Boyle, E. A.: Zinc, chromium, vanadium and iron in the Mediterranean Sea, Deep Sea Res. A, 35, 1319–1334, https://doi.org/10.1016/0198-0149(88)90085-4, 1988.

Smedley, P. L., and Kinniburgh, D. G.: Molybdenum in natural waters: A review of occurrence, distributions and controls, Appl. Geochem. 84, 387–432. http://dx.doi.org/10.1016/j.apgeochem.2017.05.008, 2017.

Stortini, A. M., Cincinelli, A., Degli Innocenti, N., Tovar-Sánchez, A. and Knulst, J.: 1.12 - Surface Microlayer, In: Comprehensive Sampling and Sample Preparation - Vol. 1: Sampling Theory and Methodology, Pawliszyn, J. (Ed.-in-Chief), 223–246, Academic Press, Oxford, https://doi.org/10.1016/B978-0-12-381373-2.00018-1, 2012.

Ternon, E., Guieu, C., Loÿe-Pilot, M. D., Leblond, N., Bosc, E., Gasser, B., Miquel, J. C., Martin, J.: The impact of Saharan dust on the particulate export in the water column of the North Western Mediterranean Sea, Biogeosciences, 7, 809–826, https://doi.org/10.5194/bg-7-809- 2010, 2010.

The Mermex Group, et al.: Marine ecosystems' responses to climatic and anthropogenic forcings in the Mediterranean, Prog. Oceanogr., 91, 97–166, https://doi.org/10.1016/j.pocean.2011.02.003, 2011.

Theodosi, C., Markaki, Z., Tselepides, A., and Mihalopoulos, N.: The significance of atmospheric inputs of soluble and particulate major and TMs to the Eastern Mediterranean Sea, Mar. Chem. 120, 154–163, https://doi.org/10.1016/J.MARCHEM.2010.02.003, 2010.

Thieuleux, F., Moulin, C., Bréon, F. M., Maignan, F., Poitou, J., and Tanré, D.: Remote sensing of aerosols over the oceans using MSG/SEVIRI imagery, Ann. Geophys., 23, 3561–3568, https://doi.org/10.5194/angeo-23-3561-2005, 2005.

Tovar-Sánchez, A., Arrieta, J. M., Duarte, C. M., and Sañudo-Wilhelmy, S. A.: Spatial gradients in trace metal concentrations in the surface microlayer of the Mediterranean Sea, Front. Mar. Sci., 1, 79, https://doi.org/10.3389/fmars.2014.00079, 2014.

Tovar-Sánchez, A., González-Ortegón, E., and Duarte, C. M.: Trace metal partitioning in the top meter of the ocean, Sci. Total Environ., 652, 907–914, https://doi.org/10.1016/j.scitotenv.2018.10.315, 2019.

Tovar-Sánchez, A., Rodríguez-Romero, A., Engel, A., Zäncker, B., Fu, F., Marañón, E., Pérez-Lorenzo, M., Bressac, M., Wagener, T., Triquet, S., Siour, G., Desboeufs, K., and Guieu, C.: Characterizing the surface microlayer in the Mediterranean Sea: trace metal concentrations and microbial plankton abundance, Biogeosciences, 17, 2349–2364, https://doi.org/10.5194/bg-17-2349-2020, 2020.

Travnikov,O., Ilyin I., O.Rozovskaya, M.Varygina, W.Aas, H.T.Uggerud, K. Mareckova, and R. Wankmueller, Long-term Changes of Heavy Metal Transboundary Pollution of the Environment (1990-2010), EMEP Status Report 2/2012, 2012.

Van Wambeke, F., Pulido, E., Catala, P., Dinasquet, J., Djaoudi, K., Engel, A., Garel, M., Guasco, S., Marie, B., Nunige, S., Taillandier, V., Zäncker, B., and Tamburini, C.: Spatial patterns of ectoenzymatic kinetics in relation to biogeochemical properties in the Mediterranean Sea and the concentration of the fluorogenic substrate used, Biogeosciences, 18, 2301–2323, https://doi.org/10.5194/bg-18-2301-2021, 2021a.

Van Wambeke, F., Taillandier, V., Desboeufs, K., Pulido-Villena, E., Dinasquet, J., Engel, A., Marañón, E., Ridame, C., and Guieu, C.: Influence of atmospheric deposition on biogeochemical cycles in an oligotrophic ocean system, Biogeosciences, 18, 5699–5717, https://doi.org/10.5194/bg-18-5699-2021, 2021b..

Vincent, J., Laurent, B., Losno, R., Bon Nguyen, E., Roullet, P., Sauvage, S., Chevaillier, S., Coddeville, P., Ouboulmane, N., di Sarra, A. G., Tovar-Sánchez, A., Sferlazzo, D., Massanet, A., Triquet, S., Morales Baquero, R., Fornier, M., Coursier, C., Desboeufs, K., Dulac, F., and Bergametti, G.: Variability of mineral dust deposition in the western Mediterranean basin and south-east of France, Atmos. Chem. Phys., 16, 8749–8766, https://doi.org/10.5194/acp-16-8749-2016, 2016.

Violaki, K., Bourrin, F., Aubert, D., Kouvarakis, G., Delsaut, N., and Mihalopoulos, N.: Organic phosphorus in atmospheric deposition over the Mediterranean Sea: An important missing piece of the phosphorus cycle, Prog. Oceanogr., 163, 50–58, https://doi.org/10.1016/j.pocean.2017.07.009, 2018.

Wagener, T., Pulido-Villena, E., and Guieu, C.: Dust iron dis-solution in seawater:Results from a one-year time-series in the Mediterranean Sea, Geophys. Res. Lett., 35, L16601, https://doi.org/10.1029/2008GL034581, 2008.

Wagener, T., Guieu, C., and Leblond, N.: Effects of dust deposition on iron cycle in the surface Mediterranean Sea: results from a mesocosm seeding experiment, Biogeosciences, 7, 3769–3781, https://doi.org/10.5194/bg-7-3769-2010, 2010.

Weinzierl, B., Ansmann, A., Prospero, J. M., Althausen, D., Benker, N., Chouza, F., Dollner, M., Farrell, D., Fomba, W. K., Freudenthaler, V., Gasteiger, J., Groß, S., Haarig, M., Heinold, B., Kandler, K., Kristensen, T. B., Mayol-Bracero, O. L., Müller, T., Reitebuch, O., Sauer, D., Schäfler, A., Schepanski, K., Spanu, A., Tegen, I., Toledano, C., & Walser, A.. The Saharan Aerosol Long-Range Transport and Aerosol–Cloud-Interaction Experiment: Overview and Selected Highlights, BAMS, 98(7), 1427-1451, https://doi.org/10.1175/BAMS-D-15-00142.1, 2017.

Wurl, O.: Practical Guidelines for the Analysis of Seawater, 1st ed., CRC Press., 2009.

Wuttig, K., Wagener, T., Bressac, M., Dammshäuser, A., Streu, P., Guieu, C., and Croot, P. L.: Impacts of dust deposition on dissolved trace metal concentrations (Mn, Al and Fe) during a mesocosm experiment, Biogeosciences, 10, 2583–2600, https://doi.org/10.5194/bg-10-2583-2013, 2013.

Yoon, Y. Y., Martin, J.-M., and Cotté, M. H.: Dissolved trace metals in the western Mediterranean Sea: total concentration and fraction isolated by C18 Sep-Pak technique, Mar. Chem., 66, 129–148, https://doi.org/10.1016/S0304-4203(99)00033-X,1999.

Figure Captions:

Figure 1: Sampling chronology during the ION and FAST stations for the ML and rains. The blue periods correspond to rainfall in the vicinity of the R/V position (from ERA 5 reanalysis and radar imagery, see section 3.1.), and blue triangles to the rainfall on the R/V position. Samplings were performed 4 days (ML25) and 2 days (ML27) before and 2 h (ML29) after Rain ION, and at a higher frequency at FAST station: 57 (ML02), 37 (ML03) and 7.5 (ML04) hours before and 4.5 (ML05+4), 12 (ML05+12), 24 hours (ML06) after Rain FAST.

Figure 2: Total precipitation (mm) between 28 May at 20:00 UTC and 29 May 2017 at 10:00 UTC (Rain ION, left figure) and between the 4 June at 20:00 and 5 June 2017 at 09:00 UTC (Rain FAST right figure) from ERA5 ECMWF reanalysis. The red circle indicates the R/V position.

Figure 3: On-board lidar-derived: apparent backscatter coefficient (ABC) (top panel), temporal evolution of the lidar-derived volume depolarization ratio (VDR) (middle panel in local time) where the dust plume is highlighted for values higher than ~1.7 (yellow to red colours) and the rain by values higher than 3 (indicated by the white arrow), and vertical profiles of the aerosol extinction coefficient in cloud free condition, integrated over 3 periods, noted 1, 2 and 3 on the top panel, along the dust plume event (bottom panels). The grey shade represents the root mean square (rms) variability along the time of the measurement. The dust layer is highlighted on the profiles. The mean aerosol optical thickness is given in the boxed legend with its temporal variability (1 sigma). The location of the marine boundary layer (MBL) is also pointed.

Figure 4: Rain rates (mm/h) during the night between the 4 and 5 June, when Rain FAST was collected on-board, issued from European rain radar composites (OPERA programme) of 5 June between 00:00 and 02:45 UTC.

Figure 5: Box plots of dissolved (upper panels) and particulate (middle panels) marine concentrations (pM) and Kd values (lower panels) for the different TMs within the ML at ION (right panels) and FAST (left panels). In the box plots, the box indicates the interquartile range, i.e. the 25th and the 75 th percentile, and the line within the box marks the median. The whiskers indicate the quartiles ±1.5 times the interquartile range. Points above and below the whiskers indicate outliers outside the 10th and 90th percentile.

Figure 6: Comparison of dissolved (D) and total (T) TM concentrations to previous studies in the eastern and western Mediterranean Sea.

Figure 7: Enrichment Factors (EF, upper panel) and solubility (%, bottom panel) of phosphorus (P) and TMs ordered by increasing EF in the two rainwater samples.

Figure 8: Dissolved (upper panels) and particulate (middle panels) wet deposition fluxes (µmol m^{-2}), and Kd (lower panels) for the different TMs estimated from the two rains sampled on-board, considering the standard deviation on the TM concentrations and the spatial variability of total precipitation over the area of sampling (Rain ION in blue and Rain FAST in red). Note different scales on the y axes and that Kd value for Ti (115) in Rain FAST is out of scale.

Figure 9: Comparison between TM wet deposition fluxes (dark blue) and TM marine stock deltas (before and after the rain) in the ML (light blue) at FAST. Dissolved = upper panels and particulate = lower panels. Marine stocks increase are expressed in absolute values (Cd, Co and Pb stocks and fluxes in nmol m^{-2}, and the other TMs in µmol m^{-2}) and in relative values (%). N.E.: not enhanced (increase <5%).

Figure 10: Comparison of marine stocks in the ML at all the stations occupied during the PEACETIME cruise (light blue boxes) with atmospheric deposition fluxes estimated (1) from ION and FAST rains (dark blue boxes) and (2) from an intense wet dust deposition event of 9 g m^{-2} (blue dots). Cd, Co and Pb stocks and fluxes are in nmol m^{-2}, and the other TMs in µmol m^{-2}. For Mn, marine stocks are derived from surface concentrations close to Corsica coasts (Wuttig et al., 2013: samples OUT at 0, 5 and 10 m) and in the Ionian Sea (Saager et al., 1993: Bannock basin at 0, 10, and 15 m), as no measurement is available from the PEACETIME cruise. Boxes and whiskers as in Fig. 4.